

1 Neural signatures of vigilance decrements predict behavioural errors before they occur  
2  
3

4 Hamid Karimi-Rouzbahani<sup>1</sup>, Alexandra Woolgar<sup>\*1,2</sup>, Anina N. Rich<sup>\*1</sup>

5 <sup>1</sup>Perception in Action Research Centre and Department of Cognitive Science, Faculty of Human  
6 Sciences, Macquarie University, Australia

7 <sup>2</sup>Medical Research Council Cognition and Brain Sciences Unit, University of Cambridge, UK

8 \* Equally contributing authors

9 **Abstract-** There are many monitoring environments, such as railway control, in which lapses of  
10 attention can have tragic consequences. Problematically, sustained monitoring for rare targets is  
11 difficult, with more misses and longer reaction times over time. What changes in the brain underpin  
12 these “vigilance decrements”? We designed a multiple-object monitoring (MOM) paradigm to  
13 examine how the neural representation of information varied with target frequency and time  
14 performing the task. Behavioural performance decreased over time for the rare target (monitoring)  
15 condition, but not for a frequent target (active) condition. This was mirrored in the neural results:  
16 there was weaker coding of critical information during monitoring versus active conditions. We  
17 developed new analyses that can predict behavioural errors from the neural data more than a  
18 second before they occurred. This paves the way for pre-empting behavioural errors due to lapses in  
19 attention and provides new insight into the neural correlates of vigilance decrements.

## 20 **Introduction**

21 When people monitor displays for rare targets, they are slower to respond and more likely to miss  
22 those targets relative to frequent target conditions (Wolfe et al., 2005; Warm et al., 2008; Rich et al.,  
23 2008). This effect is more pronounced as the time doing the task increases, which is often called a  
24 ‘vigilance decrement’. Theoretical accounts of vigilance decrements fall into two main categories.  
25 ‘Cognitive depletion’ theories suggest performance drops as cognitive resources are ‘used up’ by the  
26 difficulty of sustaining attention under vigilance conditions (Helton et al., 2008; Helton et al., 2011;  
27 Warm et al., 2008). In contrast, ‘mind wandering’ theories suggest that the boredom of the task

28 tends to result in insufficient involvement of cognitive resources, which in turn leads to performance  
29 decrements (Manly et al., 1999; Smallwood et al., 2006; Young et al., 2002). Either way, there are  
30 many real-life situations where such a decrease in performance over time can lead to tragic  
31 consequences, such as the Paddington railway disaster (UK, 1999), in which a slow response time to  
32 a stop signal resulted in a train moving another 600 meters past the signal into the path of an  
33 oncoming train. With the move towards automated and semi-automated systems in many high-risk  
34 domains (e.g., power-generation and trains), humans now commonly need to monitor systems for  
35 infrequent computer failures or errors. These modern environments challenge our attentional  
36 systems and make it urgent to understand the way in which monitoring conditions change the way  
37 important information about the task is encoded in the human brain.

38

39 To date, most vigilance and rare target studies have used simple displays with static stimuli.  
40 Traditional vigilance tasks, inspired by radar operators in WWII (Mackworth, 1948), require  
41 participants to respond to infrequent visual events on otherwise blank screens (Temple et al., 2000).  
42 Contemporary vigilance tasks, like the Sustained Attention to Response Task (SART), require  
43 participants to respond frequently to a rapid stream of static displays and occasionally withhold a  
44 response (Rosvold et al., 1956; Rosenberg et al., 2013). However, modern environments (e.g., rail  
45 and air traffic control) have additional challenges not encapsulated by these measures. This includes  
46 multiple moving objects, potentially appearing at different times, and moving simultaneously in  
47 different directions. When an object moves in the space, its neural representation has to be  
48 continuously updated so we can perceive the object as having the same identity. Tracking moving  
49 objects also requires considerable neural computation: in addition to spatial remapping, for  
50 example, we need to predict direction, speed, and the distance of the object to a particular  
51 destination. These features cannot be studied using static stimuli; they require objects that shift  
52 across space over time. In addition, operators have complex displays requiring selection of some

53 items while ignoring others. We therefore need new approaches to study vigilance decrements in  
54 situations that more closely resemble the real-life environments in which humans are now  
55 operating. Developing these methods will provide a new perspective on fundamental questions of  
56 how the brain implements sustained attention in moving displays, and the way in which monitoring  
57 compared with active task involvement changes the encoding of task information. These new  
58 methods may also provide avenues to optimise performance in high-risk monitoring environments.

59

60 The brain regions involved in maintaining attention over time has been studied using functional  
61 Magnetic Resonance Imaging (fMRI), which measures changes in cerebral blood flow (Adler et al.,  
62 2001; Benedict et al., 2002; Coull et al., 1996; Gilbert et al., 2006; Johannsen et al., 1997; Ortuno et  
63 al., 2002; Perin et al., 2010; Scnall et al., 2007; Sturm et al., 1999; Tana et al., 2010; Thakral et al.,  
64 2009; Wingen et al., 2008). These studies compared brain activation in task vs. resting baseline or  
65 sensorimotor control (which involved no action) conditions and used univariate analyses to identify  
66 regions with higher activation under task conditions. This has the limitation that there are many  
67 features that differ between the contrasted (subtracted) conditions, not just the matter of sustained  
68 attention. Specifically, this comparison cannot distinguish whether the activation during sustained  
69 attention is caused by the differences in the task, stimuli, responses or a combination of these  
70 factors. As it is challenging to get sufficient data from monitoring (vigilance) tasks in the scanner,  
71 many previous studies used tasks with relatively frequent targets, in which vigilance decrements  
72 usually do not occur. However, despite these challenges, Langner et al. (2013) reviewed vigilance  
73 neuroimaging studies and identified a network of right-lateralized brain regions including  
74 dorsomedial, mid- and ventrolateral prefrontal cortex, anterior insula, parietal and a few subcortical  
75 areas that they argue form the core network subserving vigilant attention in humans. The areas  
76 identified by Langner et al. (2013) show considerable overlap with a network previously identified as  
77 being recruited by many cognitively challenging tasks, the 'multiple demand' (MD) regions, which

78 include the right inferior frontal gyrus, anterior insula and intra parietal sulcus (Duncan & Owen,  
79 2000; Duncan, 2010; Fedorenko et al., 2013; Woolgar et al., 2011; Woolgar et al., 2015a; Woolgar et  
80 al., 2015b).

81

82 Other fMRI studies of vigilance have focused on the default mode network, composed of discrete  
83 areas in the lateral and medial parietal, medial prefrontal, and medial and lateral temporal cortices  
84 such as posterior cingulate cortex (PCC) and ventral anterior cingulate cortex (vACC), which is  
85 thought to be active during 'resting state' and less active during tasks (Greicius et al., 2003; Greicius  
86 et al., 2009; Raichle et al., 2015). Eichele et al., (2008) suggested that lapses in attention can be  
87 predicted by decrease of deactivation of this default mode network. In contrast, Weissman et al.  
88 (2006) identified deactivation in the anterior cingulate and right prefrontal regions in pre-stimulus  
89 time windows when targets were missed. More recently, Sadaghiani et al. (2015) showed that the  
90 functional connectivity between sensory and 'vigilance-related' (Cingulo-Opercular) brain areas  
91 decreased prior to behavioural misses in an auditory task while the connectivity increased between  
92 the same sensory area and the default-mode network. These suggest that modulation of  
93 interactions between sensory and vigilance-related brain areas might be responsible for behavioural  
94 misses in monitoring tasks.

95

96 Detecting changes in brain activation that correlate with lapses of attention can be particularly  
97 challenging with fMRI, given that it has poor temporal resolution. Electroencephalography (EEG),  
98 which records electrical activity at the scalp, has much better temporal resolution, and has been the  
99 other major approach for examining changes in brain activity during sustained attention tasks.  
100 Frequency band analyses have shown that low-frequency alpha (8 to 10.9 Hz) oscillations predict  
101 task workload and performance during monitoring of simulated air traffic (static) displays with rare  
102 targets, while frontal theta band (4 to 7.9 Hz) activity predicts task workload only in later stages of

103 the experiment (Kamzanova et al., 2014). Other studies find that increases in occipital alpha  
104 oscillations can predict upcoming error responses (Mazaheri et al., 2009) and misses (O'Connell et  
105 al., 2009) in go/no-go visual tasks with target frequencies of 11% and 9%, respectively. These  
106 changes in signal power that correlate with the task workload or behavioural outcome of trials are  
107 useful, but provide relatively coarse-level information about what changes in the brain during  
108 vigilance decrements.

109

110 Understanding the neural basis of decreases in performance over time under vigilance conditions is  
111 not just theoretically important, it also has potential real-world applications. In particular, if we  
112 could identify a reliable neural signature of attentional lapses, then we could potentially intervene  
113 prior to any overt error. For example, with the development of autonomous vehicles, being able to  
114 detect when a driver is not engaged, combined with information about a potential threat, could  
115 allow emergency braking procedures to be initiated. Previous studies have used physiological  
116 measures such as pupil size (Yoss, et al., 1970), body temperature (Molina et al., 2019), skin  
117 conductance, blood pressure, etc. (Lohani et al., 2019) to indicate the level of human arousal or  
118 alertness, but these lack the fine-grained information necessary to distinguish transient dips from  
119 problematic levels of inattention in which task-related information is lost. In particular, we lack  
120 detail on how information processing changes in the brain during vigilance decrements. This  
121 knowledge is crucial to develop a greater theoretical and practical understanding of how humans  
122 sustain vigilance.

123

124 In this study, we developed a new task, multiple object monitoring (MOM), which includes key  
125 features of real-life situations confronting human operators in high-risk environments. These  
126 features include moving objects, varying levels of target frequency, and a requirement to detect and  
127 avoid collisions. We recorded neural data using the highly-sensitive method of

128 magnetoencephalography (Baillet, 2017) and used multivariate pattern analyses (MVPA) to detect  
129 changes in information encoded in the brain. We used these new approaches to better understand  
130 the way in which changes between active and monitoring tasks affects neural processing, including  
131 functional connectivity. We then examined the potential for using these neural measures to predict  
132 forthcoming behavioural misses based on brain activity.

133

## 134 Methods

### 135 Participants:

136 We tested twenty-one right-handed participants (10 male, 11 female, mean age = 23.4 years (SD =  
137 4.7 years), all Macquarie University students) with normal or corrected to normal vision. The Human  
138 Research Ethics Committee of Macquarie University approved the experimental protocols and the  
139 participants gave informed consent before participating in the experiment. We reimbursed each  
140 participant AU\$40 for their time completing the MEG experiment, which lasted for about 2 hours  
141 including setup.

142

143

### 144 Apparatus:

145 We recorded neural activity using a whole-head MEG system (KIT, Kanazawa, Japan) with 160 coaxial  
146 first-order gradiometers, at a sampling rate of 1000 Hz. We projected the visual stimuli onto a mirror  
147 at a distance of 113 cm above participants' heads while they were in the MEG. An InFocus IN5108  
148 LCD back projection system (InFocus, Portland, Oregon, USA), located outside the magnetically  
149 shielded room, presented the dynamically moving stimuli, controlled by a desktop computer  
150 (Windows 10; Core i5 CPU; 16 GB RAM; NVIDIA GeForce GTX 1060 6GB Graphics Card) using

151 MATLAB with Psychtoolbox 3.0 extension (Brainard, 1997; Kleiner et al., 2007). We set the refresh  
152 rate of the projector at 60 Hz and used parallel port triggers and a photodiode to mark the beginning  
153 (dot appearing on the screen) and end (dot disappearing off the screen) of each trial. We recorded  
154 participant's head shape using a pen digitizer (Polhemus Fastrack, Colchester, VT) and placed five  
155 marker coils on the head which allowed the location of the head in the MEG helmet to be monitored  
156 during the recording- we checked head location at the beginning, half way through and the end of  
157 recording. We used a fibre optic response pad (fORP, Current Designs, Philadelphia, PA, USA) to  
158 collect responses and an EyeLink 1000 MEG-compatible remote eye-tracking system (SR Research,  
159 1000 Hz monocular sampling rate) to record eye position. We focused the eye-tracker on the right  
160 eye of the participant and calibrated the eye-tracker immediately before the start of MEG data  
161 recording.

162

### 163 Task and Stimuli:

164 *Task summary:* The task was to avoid collisions of relevant moving dots with the central object by  
165 pressing the space bar if the dot passed a deflection point in a visible predicted trajectory without  
166 changing direction to avoid the central object (see Figure 1A; a demo can be found here  
167 <https://osf.io/c6hy9/>). A text cue at the start of each block indicated which colour of dot was  
168 relevant for that block. The participant only needed to respond to targets in this colour; dots in the  
169 other colour formed distractors. Pressing the button deflected the dot in one of two possible  
170 directions (counterbalanced) to avoid collision.

171

172 *Stimuli:* The stimuli were moving dots in one of two colours that followed visible trajectories and  
173 covered a visual area of  $3.8 \times 5$  degrees of visual angle (dva; Figure 1A). We presented the stimuli in  
174 blocks of 110 s duration, with at least one dot moving on the screen at all times during the 110s  
175 block. The trajectories directed the moving dots from two corners of the screen (top left and bottom

176 right) straight towards a centrally presented static “object” (a white dot of 0.25 dva) and then  
177 deflected away (either towards the top right or bottom left of the screen; in pathways orthogonal to  
178 their *direction of approach*) from the static object at a set distance (the deflection point).

179

180 Target dots deviated from the visible trajectory at the deflection point and continued moving  
181 towards the central object. The participant had to push the space bar to prevent a ‘collision’. If the  
182 response was made before the dot reached the centre of the object, the dot deflected, and this was  
183 counted as a ‘hit’. If the response came after this point, the dot continued straight, and this was  
184 counted as a ‘miss’, even if they pressed the button before the dot totally passed through central  
185 object.

186

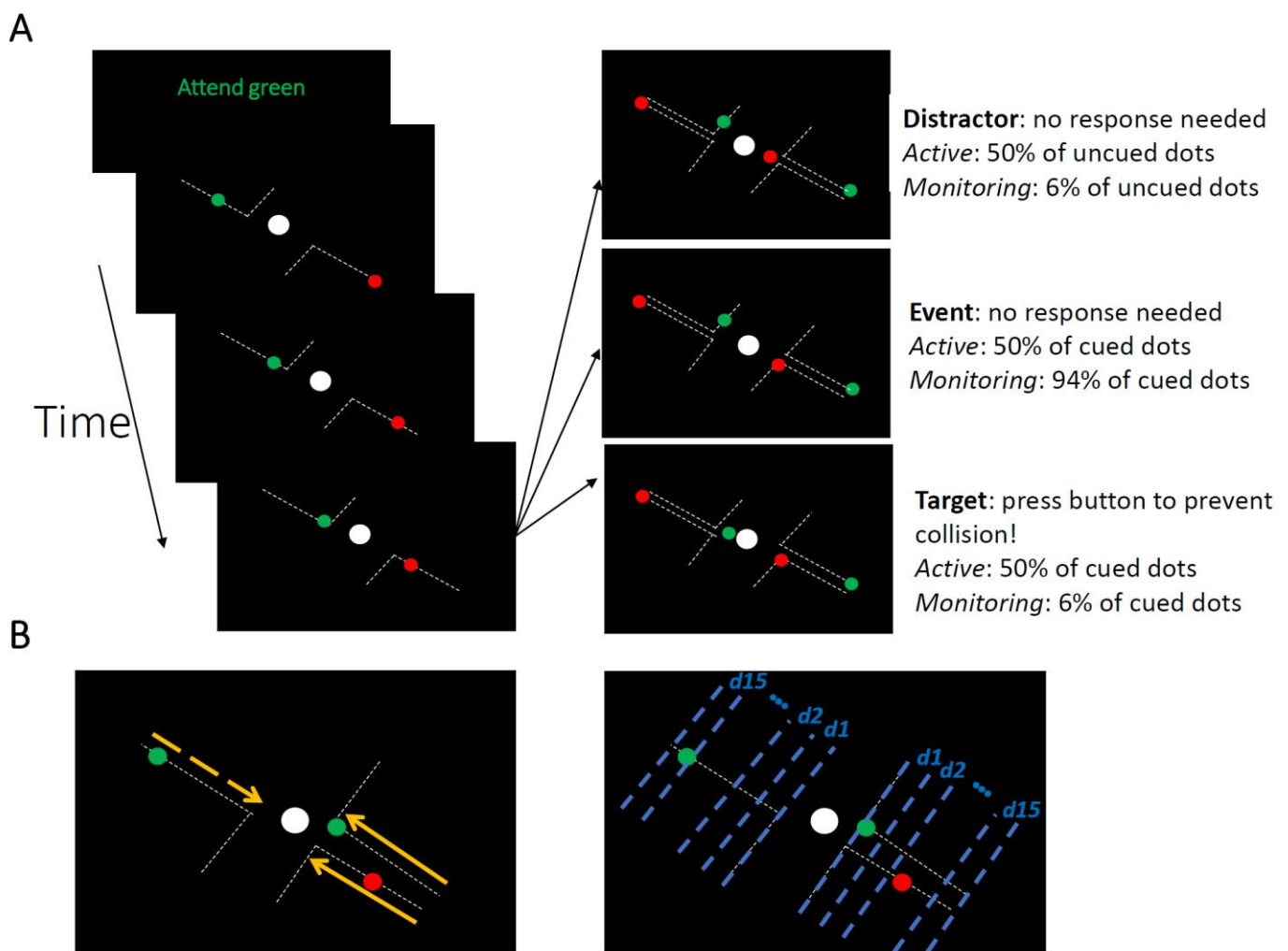


Figure 1. The Multiple Object Monitoring (MOM) task and types of information decoded. (A) At the start of a block, the relevant colour is cued (here, green; distractors in red). Over the on-task period (~30 mins per task condition), multiple dots entered from either direction, each moving along a visible individual trajectory towards the middle object. Only attended dots that failed to deflect along the trajectories at the deflection point required a response (Target: bottom right display). Participants did not need to press the button for the unattended dot (Distractor: top right display) and the dots that kept moving on the trajectories (Event: middle right panel). Each dot took ~1226 ms from appearance to deflection. (B) Direction of approach information (left display: left vs. right as indicated by dashed and solid lines, respectively) and distance information (right display). Note the blue dashed lines and orange arrows were not present in the actual display. A demo of the task can be found here <https://osf.io/c6hv9/>.

187

188 The time from dot onset in the periphery to the point of deflection was  $1226 \pm 10$  (Mean  $\pm$  SD)  
 189 milliseconds. Target (and distractor event) dots took  $410 \pm 10$  (Mean  $\pm$  SD) milliseconds to cross from  
 190 the deflection point to the collision point. In total, each dot moved across the display for  $2005 \pm 12$   
 191 (Mean  $\pm$  SD) milliseconds before starting to fade away after either deflection or travel through the  
 192 object. The time delay between the onsets of different dots (ISI) was  $1660 \pm 890$  (Mean  $\pm$  SD)

193 milliseconds. There were 1920 dots presented in the whole experiment (~56 mins). Each 110 second  
194 block contained 64 dots, 32 (50%) in red and 32 (50%) in green, while the central static object and  
195 trajectories were presented in white on a black background.

196

197 *Conditions:* There were two target frequency conditions. In 'Monitoring' blocks, target dots were  
198 ~6.2% of cued-colour dots (2 out of 32 dots). In 'Active' blocks, target dots were 50% of cued-colour  
199 dots (16 out of 32 dots). The same proportion of dots in the non-cued colour failed to deflect; these  
200 were distractors (see Figure 1A, top right panel). Participants completed two practice blocks of the  
201 Active condition and then completed 30 blocks in the main experiment (15 Active followed by 15  
202 Monitoring or *vice versa*, counterbalanced across participants).

203

204 The time between the appearance of target dots varied unpredictably, with distractors and  
205 correctly-deflecting dots (events) intervening. In Monitoring blocks, there was an average time  
206 between targets of 57.88 ( $\pm 36.03$  SD) seconds. In Active blocks, there was an average time between  
207 targets of 7.20 ( $\pm 6.36$  SD) seconds.

208

209 *Feedback:* On target trials, if the participant pressed the space bar in time, this 'hit' was indicated by  
210 a specific tone and deflection of the target dot. There were three types of potential false alarm, all  
211 indicated by an error tone and no change in the trajectory of the dot. These were if the participant  
212 responded: (1) too early, while the dot was still on the trajectory; (2) when the dot was not a target  
213 and had been deflected automatically ('event' in Figure 1A, middle right); or (3) when the dot was in  
214 the non-cued colour ('distractor' in Figure 1A, top right) in any situation. Participants had only one  
215 chance to respond per dot; any additional responses resulted in 'error' tones. As multiple dots could

216 be on the screen, we always associated the button press to the dot which was closest to the central  
217 object.

218

219 [Pre-processing:](#)

220 MEG data were filtered online using band-pass filters in the range of 0.03 to 200 Hz and notch-  
221 filtered at 50 Hz. We did not perform eye-blink artefact removal because it has been shown that  
222 blink artefacts are successfully ignored by multivariate classifiers as long as they are not  
223 systematically different between decoded conditions (Grootswagers et al., 2017). We then imported  
224 the data into Matlab and epoched them from -100 to 3000 ms relative to the trial onset time. Finally,  
225 we down-sampled the data to 200 Hz for the decoding of our two key measures: *direction of*  
226 *approach* and *distance to object* (see below).

227

228 [Multivariate pattern analyses \(MVPA\):](#)

229 We measured the information contained in the multivariate (multi-sensor) patterns of MEG data by  
230 training a linear discriminant analysis (LDA) classifier using a set of training trials from two categories  
231 (e.g., for the *direction of approach* measure, this was dots approaching from left vs. right, see  
232 below). We then tested to see whether the classifier could predict the category of an independent  
233 (left-out) set of testing data from the same participant. We used a 10-fold cross-validation approach,  
234 splitting the data into training and testing subsets. Specifically, we trained the LDA classifier on 90%  
235 of the trials and tested it on the left-out 10% of the trials. This procedure was repeated 10 times  
236 each time leaving out a different 10% subset of the data for testing (i.e., 10-fold cross validation).

237

238 We decoded two major task features from the neural data: (1) the *direction of approach* (left vs.  
239 right); and (2) the distance of each moving dot from the centrally fixed object (*distance to object*),

240 which correspond to visual (retinal) information changing over time. Our interest was in the effect of  
241 selective attention (attended vs. unattended) and Target Frequency conditions (Active vs.  
242 Monitoring) on the neural representation of this information, and how the representation of  
243 information changed on trials when participants missed the target.

244

245 We decoded left vs. right *directions of approach* (as indicated by yellow arrows in Figure 1B) every 5  
246 ms starting from 100 ms before the appearance of the dot on the screen to 3000 ms later. Please  
247 note that as each moving dot is considered a trial, trial time windows (epochs) overlapped for 62.2%  
248 of trials. In Monitoring blocks, 1.2% of target trials overlapped (two targets were on the screen  
249 simultaneously but lagged relative to one another). In Active blocks, 17.1% of target trials  
250 overlapped.

251

252 For the decoding of *distance to object*, we split the trials into the time windows corresponding to 15  
253 equally spaced distances of the moving dot relative to the central object (as indicated by blue lines in  
254 Figure 1B), with distance 1 being closest to the object, and 15 being furthest away (the dot having  
255 just appeared on the screen). Next, we collapsed (concatenated) the MEG signals from identical  
256 distances (splits) across both sides of the screen (left and right), so that every distance included data  
257 from dots approaching from both left and right side of the screen. This concatenation ensures that  
258 distance information decoding is not affected by the *direction of approach*. Finally, we trained and  
259 tested a classifier to distinguish between the MEG signals (a vector comprising data from all MEG  
260 sensors, concatenated over all time points in the relevant time window), pertaining to each pair of  
261 distances (e.g., 1 vs. 2) using a leave-one-out cross-validation procedure. We obtained classification  
262 accuracy for all possible pairs of distances (105 combinations of 15 distances). To obtain a single  
263 decoding value per distance, we averaged the 14 classification values that corresponded to that  
264 distance against other 14 distances. For example, the final decoding accuracy for distance 15 was an

265 average of 15 vs. 14, 15 vs. 13, 15 vs. 12 and so on until 15 vs. 1. We repeated this procedure for our  
266 main Target Frequency conditions (Active vs. Monitoring), Attention conditions (attended vs.  
267 unattended) and Time on Task (first and last five blocks of each task condition, which are called early  
268 and late blocks here, respectively). This was done separately for *correct* and *miss* trials and for each  
269 participant separately.

270

271 **Informational connectivity analysis:**

272 To evaluate possible modulations of brain connectivity between the attentional networks of the  
273 frontal brain and the occipital visual areas, we used a simplified version of our recently developed  
274 RSA-based connectivity analysis (Goddard et al., 2016; Karimi-Rouzbahani, 2018; Karimi-Rouzbahani  
275 et al., 2019). Specifically, we evaluated the informational connectivity, which measures the similarity  
276 of distance information between areas, across our main Target Frequency conditions (Active vs.  
277 Monitoring), Attention conditions (attended vs. unattended) and Time on Task (first and last five  
278 blocks of each task condition, which are called early and late blocks here, respectively). This was  
279 separately done for *correct* and *miss* trials, using representational dissimilarity matrices (RDM;  
280 Kriegeskorte et al., 2008). To construct the RDMs, we decoded all possible combinations of distances  
281 from each other yielding a 15 by 15 cross-condition classification matrix, for each condition  
282 separately. We obtained these matrices from peri-occipital and peri-frontal areas to see how the  
283 manipulation of Attention, Target Frequency and Time on Task modulated the correlation of  
284 information (RDMs) between those areas on *correct* and *miss* trials. We quantified connectivity using  
285 Spearman's rank correlation of the matrices obtained from those areas, only including the lower  
286 triangle of the RDMs (105 decoding values). To avoid bias when comparing the connectivity on  
287 *correct* vs. *miss* trials, the number of trials were equalized by subsampling the *correct* trials to the  
288 number of *miss* trials and repeating the subsampling 100 times before finally averaging them for  
289 comparison with *miss* trials.

290 [Error data analysis:](#)

291 Next, we asked what information was coded in the brain when participants missed targets. To study  
292 information coding in the brain on *miss* trials, where the participants failed to press the button when  
293 targets failed to automatically deflect, we used our recently-developed method of error data  
294 analysis (Woolgar et al., 2019). Essentially, this analysis asks whether the brain represents the  
295 information similarly on *correct* and *miss* trials. For that purpose, we trained a classifier using the  
296 neural data from a proportion of *correct* trials (i.e., when the target dot was detected and manually  
297 deflected punctually) and tested on both the left-out portion of the *correct* trials (i.e., cross-  
298 validation) and on the *miss* trials. If decoding accuracy is equal between the *correct* and *miss* trials,  
299 we can conclude that information coding is maintained on *miss* trials as it is on *correct* trials.  
300 However, if decoding accuracy is lower on *miss* trials than on *correct* trials, we can infer that  
301 information coding differs on *miss* trials, consistent with the change in behaviour. Since *correct* and  
302 *miss* trials were visually different after the deflection point, we only used data from before the  
303 deflection point.

304

305 For these error data analyses, the number of folds for cross-validation were determined based on  
306 the proportion of *miss* to *correct* trials (number of folds = number of miss trials/number of correct  
307 trials). This allowed us to test the trained classifiers with equal numbers of *miss* and *correct* trials to  
308 avoid bias in the comparison.

309

310 [Predicting behavioural performance from neural data:](#)

311 We developed a new method to predict, based on the most task-relevant information in the neural  
312 signal, whether or not a participant would press the button for a target dot in time to deflect it on a  
313 particular trial. This method includes three steps, with the third step being slightly different for the

314 left-out testing participant vs. the other 20 participants. First, for every participant, we trained 105  
315 classifiers using ~80% of correct trials to discriminate the 15 distances. Second, we tested those  
316 classifiers using half of the left-out portion (~10%) of the correct trials, which we called validation  
317 trials, by simultaneously accumulating (i.e., including in averaging) the accuracies of the classifiers at  
318 each distance and further distances as the validation dot approached the central object. The  
319 validation set allowed us to determine a decision threshold for predicting the outcome of each  
320 testing trial: whether it was a *correct* or *miss* trial. Third, we performed a second-level classification  
321 on testing trials which were the other half (~10%) of the left-out portion of the correct trials and the  
322 miss trials, using each dot's accumulated accuracy calculated as in the previous step. Accordingly, if  
323 the testing dot's accumulated accuracy was **higher** than the decision threshold, it was predicted as  
324 *correct*, otherwise *miss*. For all participants, except for the left-out testing one, the decision  
325 threshold was chosen from a range of **multiples** (0.1 to 4 in steps of 0.1) of the standard deviation  
326 below the accumulated accuracy obtained for the validation set on the second step. For determining  
327 the optimal threshold for the testing participant, however, instead of a range of multiples, we used  
328 the average of the best performing multiples (i.e., the one which predicted the behavioural outcome  
329 of the trial more accurately) obtained from the other 20 participants. This avoided circularity in the  
330 analysis.

331  
332 To give more detail on the second and third steps, when the validation/testing dots were at distance  
333 #15, we averaged the accuracies of the 14 classifiers trained to classify dots at distance #15 from all  
334 other distances. Accordingly, when the dot reached distance #14, we also included and averaged  
335 accuracies from classifiers which were trained to classify distance #14 from all other distances  
336 leading to 27 classifier accuracies. Therefore, by the time the dot reached distance #1, we had 105  
337 classifier accuracies to average and predict the behavioural outcome of the trial. Every classifier's  
338 accuracies were either 1 or 0 corresponding to correct or incorrect classification of dot's distance,

339 respectively. Note that accumulation of classifiers' accuracies, as compared to using classifier  
340 accuracy on every distance independently, provides a more robust and smoother classification  
341 measure for deciding on the label of the trials. The validation set, which was different from the  
342 testing set, allowed us to set the decision threshold based on the validation data within each subject  
343 and from the 20 participants and finally test our prediction classifiers on a separate testing set from  
344 the 21<sup>st</sup> individual participant, iteratively. The optimal threshold was 1.54 ( $\pm 0.2$ ) times the SD below  
345 the decoding accuracy on the validation set across participants.

346

347 [Eye-tracking data analysis:](#)

348 To see if we could use a less complicated physiological measure to obtain information about the  
349 processing of visual information, and to check that the decoding we observed was not just due to  
350 eye movements, we repeated the above decoding analyses using the eye-tracking data. Specifically,  
351 instead of the MEG sensor data, we decoded the information about the *direction of approach* and  
352 *distance to object* using x-y coordinates of the right eye fixation provided by the eye-tracker. All  
353 other aspects of the analysis were identical to the 'error data analysis' section. If we observe a  
354 similar decoding of information using the eye-tracking data, it would mean that we could use eye-  
355 tracking, which is a less expensive and more feasible approach for prediction of errors, instead of  
356 MEG. If the prediction from the MEG decoding was stronger than that of the eye tracking, it would  
357 mean that there was information in the neural signal over and above any artefact associated with  
358 eye movement.

359

360 [Statistical analyses:](#)

361 To determine the evidence for the null and the alternative hypotheses, we used Bayes analyses as  
362 implemented by Krekelberg (<https://klabhub.github.io/bayesFactor/>) based on Rouder et al. (2012).

363 We used standard rules for interpreting levels of evidence (Lee and Wagenmakers, 2014; Dienes,  
364 2014): Bayes factors of  $>10$  and  $<1/10$  were interpreted as strong evidence for the alternative and  
365 null hypotheses, respectively, and  $>3$  and  $<1/3$  were interpreted as moderate evidence for the  
366 alternative and null hypotheses, respectively. We interpreted the Bayes factors which fell between 3  
367 and  $1/3$  as reflecting insufficient evidence either way.

368

369 Specifically, for the behavioural data, we asked whether there was a difference between Active and  
370 Monitoring conditions in terms of miss rates and reaction times. Accordingly, we calculated the  
371 Bayes factor as the probability of the data under alternative (i.e., difference) relative to the null (i.e.,  
372 no difference) hypothesis in each block separately. In the decoding, we repeated the same  
373 procedure to evaluate the evidence for the alternative hypothesis of a difference between decoding  
374 accuracies across conditions (e.g. Active vs. Monitoring and Attended vs. Unattended) vs. the null  
375 hypothesis of no difference between them, at every time point/distance. To evaluate evidence for  
376 the alternative of above-chance decoding accuracy vs. the null hypothesis of no difference from  
377 chance, we calculated the Bayes factor between the distribution of actual accuracies obtained and a  
378 set of 1000 random accuracies obtained by randomising the class labels across the same pair of  
379 conditions (null distribution) at every time point/distance.

380

381 To evaluate the evidence for the alternative of main effects of different factors (Attention, Target  
382 Frequency and Time on Task) in decoding, we used Bayes factor ANOVA (Rouder et al., 2012). This  
383 analysis evaluates the evidence for the null and alternative hypothesis as the ratio of the Bayes  
384 factor for the full model ANOVA (i.e., including all three factors of Target Frequency, Attention and  
385 the Time on Task) relative to the restricted model (i.e., including the two other factors while  
386 excluding the factor being evaluated). For example, for evaluating the main effect of Time on Task,

387 the restricted model included Attention and Target Frequency factors but excluded the factor of  
388 Time on Task.

389

390 The priors for all Bayes factor analyses were determined based on Jeffrey-Zellner-Siow priors  
391 (Jeffreys, 1961; Zellner and Siow, 1980) which are from the Cauchy distribution based on the effect  
392 size that is initially calculated in the algorithm using a *t*-test (Rouder et al., 2012). The priors are  
393 data-driven and have been shown to be invariant with respect to linear transformations of  
394 measurement units (Rouder et al., 2012), which reduces the chance of being biased towards the null  
395 or alternative hypotheses.

396

## 397 Results

### 398 Behavioural data: The MOM task evokes a reliable vigilance decrement

399 In the first 110 second experimental block of trials (i.e., excluding the two practice blocks),  
400 participants missed 29% of targets in the Active condition and 40% of targets in the Monitoring  
401 condition. However, the number of targets in any single block is necessarily very low for monitoring  
402 conditions (for a single block, there are 16 targets for Active but only 2 targets for Monitoring). The  
403 pattern does become more robust over blocks, and Figure 2A shows the miss rates changed over  
404 time in different directions for the Active vs. Monitoring conditions. For Active blocks, miss rates  
405 decreased over the first five blocks and then plateaued at ~17%. For Monitoring, however, miss  
406 rates increased throughout the experiment: by the final block, these miss rates were up to 76% (but  
407 again, the low number of targets in Monitoring mean that we should use caution in interpreting the  
408 results of any single block alone). There was evidence that miss rates were higher in the Monitoring  
409 than Active conditions from the 4th block onwards ( $BF > 3$ ; Figure 2A). Participants' reaction times  
410 (RTs) on correct trials also showed evidence of vigilance decrements, increasing over time under

411 Monitoring but decreasing under Active task conditions (Figure 2B). There was evidence that  
412 reaction times were slower for Monitoring compared with Active from the sixth block onwards ( $BF >$   
413 3, except for Block #11). The characteristic pattern of increasing miss rates and slower RTs over time  
414 in the Monitoring relative to the Active condition validates the MOM task as effectively evoking  
415 vigilance decrements.

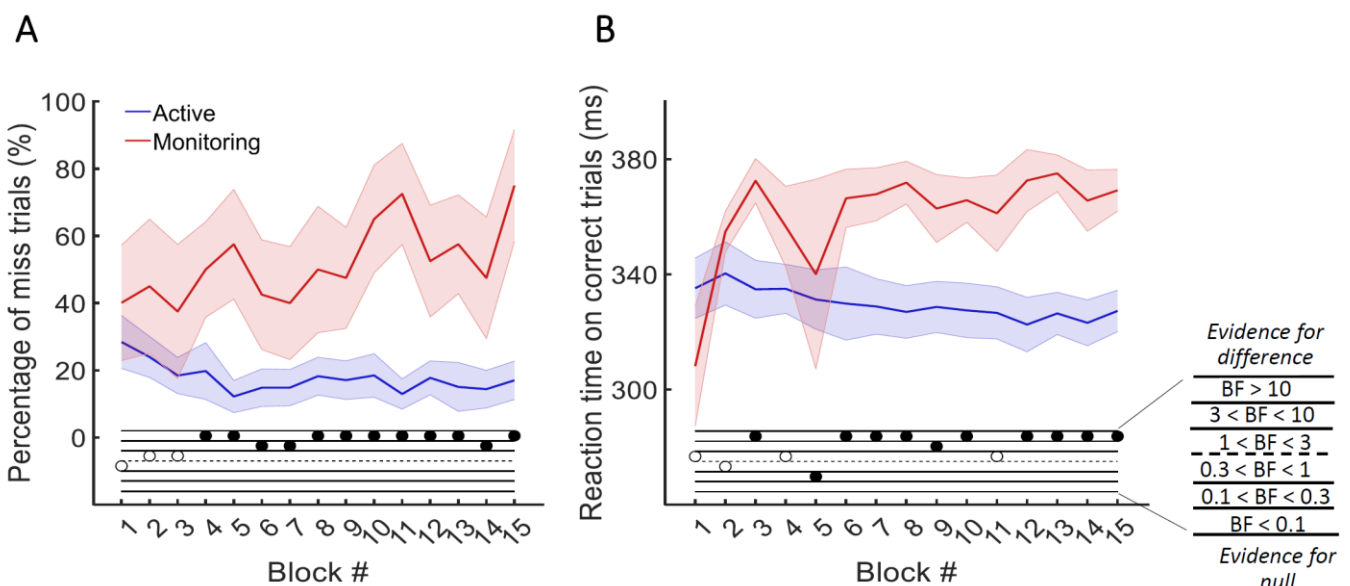


Figure 2. Behavioural performance on the MOM task. The percentage of *miss* trials (A), and *correct* reaction times (B), as a function of block. Thick lines show the average across participants (shading 95% confidence intervals) for Active (blue) and Monitoring (red) conditions. Each block lasted for 110 seconds and had either 16 (Active) or 2 (Monitoring) targets out of 32 cued-colour and 32 non-cued colour dots. Bayes Factors are shown in the bottom section of each graph: Filled circles show moderate/strong evidence for either hypothesis and empty circles indicate insufficient evidence when evaluating the contrast between Active and Monitoring conditions.

416

417 Neural data: Decoding different aspects of task-related information  
418 With so much going on in the display at one time, we first needed to verify that we can successfully  
419 decode the major aspects of the moving stimuli, relative to chance. The full data figures and details  
420 are presented in Supplementary Materials: We were able to decode both *direction of approach* and  
421 *distance to object* relative to chance from MEG signals (see Supplementary Figure 1). Thus, we can  
422 turn to our main question about how these representations were affected by the Target Frequency,  
423 Attention and Time on Task.

424

425 [The neural correlates of the vigilance decrement](#)

426 As the behavioural results showed (Figure 2), the difference between Active and Monitoring  
427 conditions increased over time, showing the greatest difference during the final blocks of the  
428 experiment. To explore the neural correlates of these vigilance decrements, we evaluated  
429 information processing in the brain during the first five and last five blocks of each task (called early  
430 and late blocks, respectively) and the interactions between the Target Frequency, Attention and the  
431 Time on Task using a 3-way Bayes factor ANOVA as explained in *Methods*.

432

433 [Effects of Target Frequency on \*direction of approach\* information](#)

434 *Direction of approach* information is a very clear visual signal ('from the left' vs 'from the right') and  
435 therefore is unlikely to be strongly modulated by other factors, except perhaps whether the dot was  
436 in the cued colour (Attended) or the distractor colour (could be ignored: Unattended). There was  
437 strong evidence for a main effect of Attention (Figure 3A;  $BF > 10$ , Bayes factor ANOVA, cyan dots)  
438 starting from 265ms and lasting until dots faded. This is consistent with maintenance of information  
439 about the attended dots and attenuation of the information about unattended dots (Supplementary  
440 Figure 1A). The large difference in coding attributable to attention remained for as long as the dots  
441 were visible.

442

443 In contrast, there was no sustained main effect of Target Frequency on the same *direction of*  
444 *approach* coding ( $0.1 < BF < 0.3$ ; Bayes factor ANOVA, Figure 3A, pink dots). For the majority of the  
445 epoch there was moderate evidence for the null hypothesis ( $BF < 1/3$ ). The sporadic time points with  
446 a main effect of Target Frequency, observed a few times before the deflection ( $3 < BF < 10$ ), likely  
447 reflect noise in the data as there is no clustering. Recall that we only focus on timepoints prior to

448 deflection, as after this point there are visual differences between Active and Monitoring, with more  
 449 dots deflecting in the Monitoring condition.

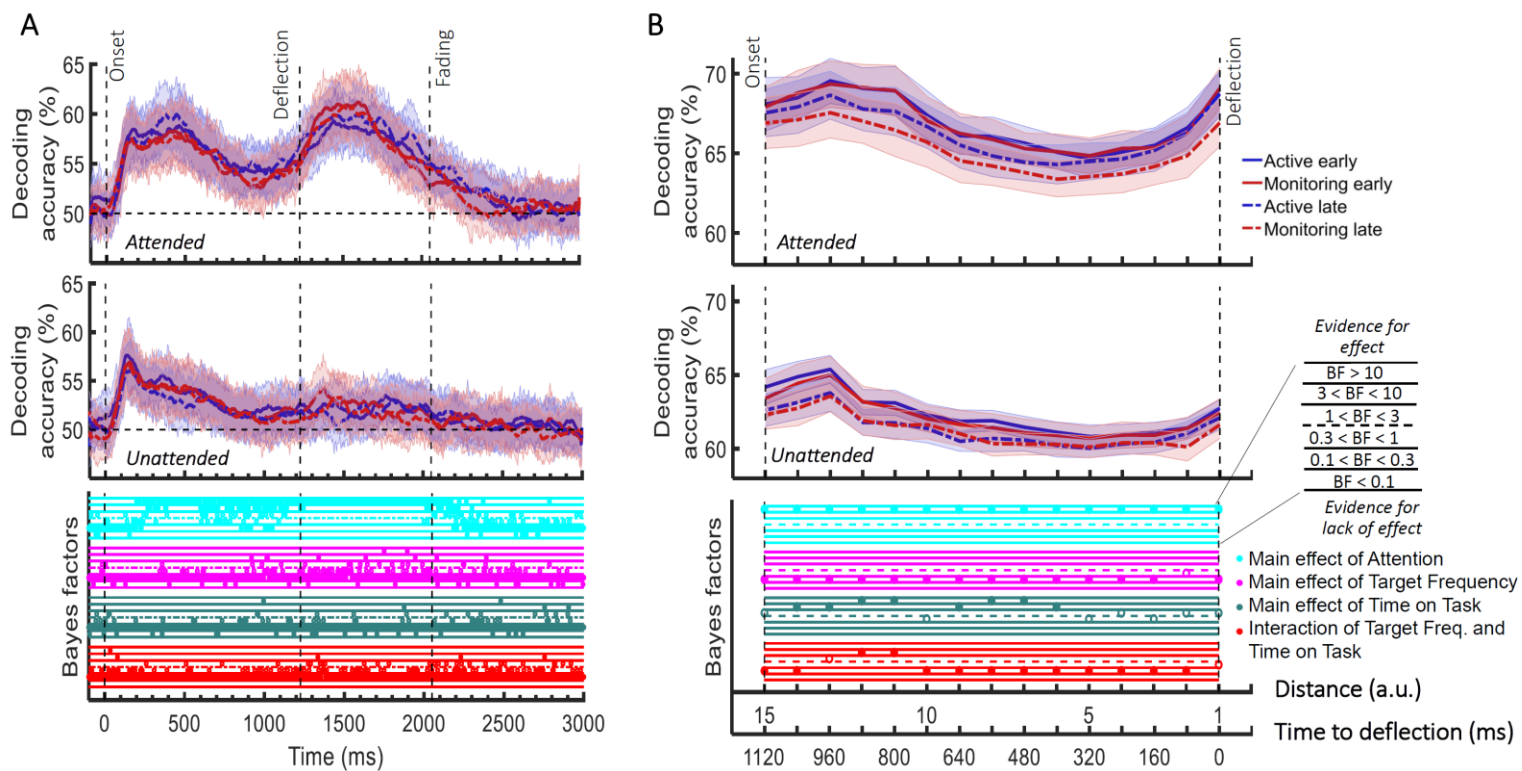


Figure 3. Impact of different conditions and their interactions on information processing on *correct* trials (all trials except those in which a target was missed or there was a false alarm). (A) Decoding of *direction of approach* information (less task-relevant). The horizontal dashed line refers to theoretical chance-level decoding (50%). Upper graph: Attended dot; Lower graph: Unattended ('distractor') dot. (B) Decoding of *distance to object* information (most task-relevant) and their Bayesian evidence for main effects and interactions. Thick lines show the average across participants (shading 95% confidence intervals). Vertical dashed lines indicate critical times in the trial. Bayes Factors are shown in the bottom section of each graph: Filled circles show moderate/strong evidence for either hypothesis and empty circles indicate insufficient evidence. Main effects and interactions of conditions calculated using Bayes factor ANOVA analysis. Cyan, pink, green and red dots indicate the main effects of Attention, Target frequency, Time on Task and the interaction between Target frequency and Time on Task, respectively. The results of Bayes factor analysis (i.e. the main effects of the three conditions and their interactions) are from the same 3-way ANOVA analysis and therefore identical for attended and unattended panels. Early = data from the first 5 blocks (~10 minutes). Late = data from the last 5 blocks (~10 minutes).

450

451 There was also no sustained main effect of the Time on Task on information about the *direction of*  
 452 *approach* ( $0.1 < BF < 0.3$ ; Bayes factor ANOVA, green dots; Figure 3A). There were no sustained 2-  
 453 way or 3-way interactions between Attention, Target Frequency and Time on Task ( $BF < 1$ ; Bayes

454 factor ANOVA). Note that the number of trials used in the training and testing of the classifiers were  
455 equalized across the 8 conditions and equalled the minimum available number of trials across those  
456 conditions shown in Figure 3. Therefore, the observed effects cannot be attributed to a difference in  
457 the number of trials across conditions.

458

#### 459 Effects of Target Frequency on critical *distance to object* information

460 The same analysis for the representation of the task-relevant *distance to object* information showed  
461 strong evidence for a main effect of Attention (BF > 10; Bayes factor ANOVA) at all 15 distances,  
462 moderate or strong evidence for a main effect of Time on Task (BF > 3; Bayes factor ANOVA) at eight  
463 of the earlier distances, and an interaction between Time on Task and Target Frequency at two of  
464 these distances (Figure 3B). There was more decoding for attended than unattended dots (compare  
465 top and bottom panels of Figure 3B). The main effect of Time on Task reflected decreased decoding  
466 in later blocks (compare dashed lines to solid lines in Figure 3B). Finally, the interaction between  
467 Target Frequency and Time on Task can be seen when comparing the solid to the dashed lines in  
468 blue and red colours, separately, and suggests a bigger decline in decoding in Monitoring compared  
469 to Active conditions. Note that as there was moderate evidence for no interaction between  
470 Attention and Target Frequency or between Attention and Time on Task ( $0.1 < BF < 0.3$ , 2-way Bayes  
471 factor ANOVA) or simultaneously between the three factors ( $BF < 0.1$ , 3-way Bayes factor ANOVA),  
472 we do not show those statistical results in the figure.

473

474 Together, these results suggest that while vigilance conditions had little or no impact on coding of  
475 the *direction of approach*, they did impact the critically task-relevant information about the distance  
476 of the dot from the object. Coding of this information declined as the time on the task increased and  
477 this effect was more pronounced when the target events happened infrequently.

478

479 Is brain connectivity modulated by Attention, Target Frequency and the Time on Task?

480 Using graph-theory-based univariate connectivity analysis, it has been recently shown that the  
481 connectivity between relevant sensory areas and “vigilance-related” cognitive areas changes prior to  
482 lapses in attention (behavioural misses; Sadaghiani et al., 2015). Therefore, we asked whether  
483 vigilance decrements across the time course of our task corresponded to changes in multi-variate  
484 connectivity, which tracks information transfer, between frontal attentional networks and sensory  
485 visual areas. Specifically, we asked whether there were changes in *information exchange* between  
486 these conditions. We used a simplified version of our method of RSA-based informational  
487 connectivity to evaluate the (Spearman’s rank) correlation between distance information RDMs  
488 across the peri-frontal and peri-occipital electrodes (see *Methods*; Goddard et al., 2016; Figure 4A).

489

490 Results showed strong evidence (Bayes factor ANOVA,  $BF = 6.3e^{21}$ ) for higher informational  
491 connectivity for Attended compared to Unattended trials, and moderate evidence for higher  
492 connectivity in Active compared to Monitoring conditions (Bayes factor ANOVA,  $BF = 3.4$ ; Figure 4B).  
493 There was insufficient evidence to determine whether there was a main effect of Time on Task  
494 (Bayes factor ANOVA,  $BF = 0.83$ ). There was moderate evidence for no 2-way and 3-way interactions  
495 between the three factors (Bayes factor ANOVA, 2-way Time on Task-Target Frequency:  $BF = 0.17$ ;  
496 Time on Task-Attention:  $BF = 0.16$ ; Target Frequency-Attention:  $BF = 0.15$ ; their 3-way interactions  
497  $BF = 0.12$ ). These results suggest that Monitoring conditions and trials in which the dots are in the  
498 distractor (unattended) colour, in which the attentional load is low, result in less informational  
499 connectivity between occipital and frontal brain areas compared to Active conditions and attended  
500 trials, respectively. This is consistent with a previous study (Alnaes et al., 2015), which suggested  
501 that large-scale functional brain connectivity depends on the attentional load, and might underpin or  
502 accompany the decrease in information decoding across the brain in these conditions (Figure 3B).

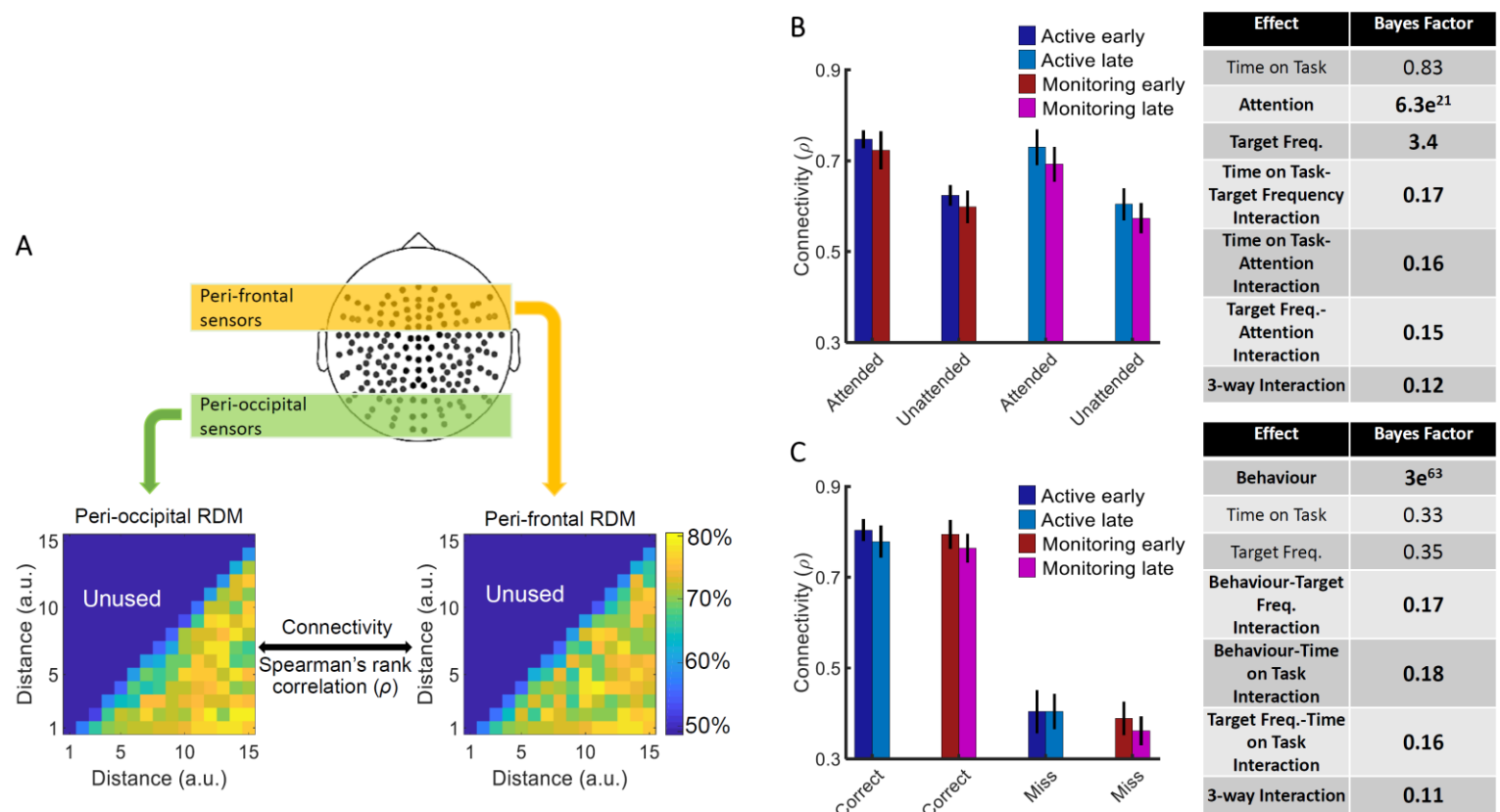


Figure 4. Relationship between informational connectivity and Attention, Target Frequency, Time on Task and the behavioural outcome of the trial (i.e., correct vs. miss). (A) Calculation of connectivity using Spearman's rank correlation between RDMs obtained from the peri-frontal and peri-occipital sensors as indicated by colored boxes, respectively. RDMs include decoding accuracies obtained from testing the 105 classifiers trained to discriminate different *distance to object* categories. (B) Connectivity values for the eight different conditions of the task and the results of three-way Bayes factor ANOVA with factors Time on Task (early, late), Attention (attended, unattended) and Target Frequency (active, monitoring), using only correct trials. (C) Connectivity values for the Active and Monitoring, Early and Late blocks of each task for *correct* and *miss* trials (attended condition only) and the result of Bayes factor ANOVA with factors Target Frequency (Active, Monitoring), Time on Task (early, late) and behavioural outcome (correct, miss) as inputs. Number of trials are equalized across conditions in B and C separately. Bars show the average across participants (error bars 95% confidence intervals). Bold fonts indicate moderate or strong evidence for either the effect or the null hypothesis.

503

504 We also compared the connectivity for the correct vs. miss trials (Figure 4C). This analysis was  
 505 performed only for attended condition as there are no miss trials for unattended condition, by  
 506 definition. There was strong evidence for less (almost half) connectivity on *miss* compared to *correct*  
 507 trials (Bayes factor ANOVA,  $BF = 3e^{63}$ ). There was insufficient evidence to determine the effects of  
 508 the Time on Task or Target Frequency (Bayes factor ANOVA,  $BF = 0.33$  and  $BF = 0.35$ , respectively)  
 509 and moderate evidence for a lack of 2-way and 3-way interactions between the three factors (Bayes

510 factor ANOVA, Behaviour-Target Frequency: BF = 0.17; Behaviour-Time on Task: BF = 0.18; Target  
511 Frequency-Time on Task: BF = 0.16; their 3-way interactions BF = 0.11). Weaker connectivity  
512 between occipital and frontal areas could have led to the behavioural misses observed in this study  
513 (Figure 1) as was previously reported in an auditory monitoring task using univariate graph-theoretic  
514 connectivity analyses (Sadaghiani et al., 2015), although, of course, these are correlational data and  
515 so we cannot make any strong causal inferences. These results cannot be explained by the number  
516 of trials as they are equalized across the 8 conditions in each of the analyses separately.

517

518 [Can we use the neural data to predict behavioural errors before they occur?](#)

519 [Is neural information processing different on \*miss\* trials?](#)

520 The results presented in Figure 3, which used only *correct* trials, showed changes due to target  
521 frequency to the representation of task-relevant information when the task was performed  
522 successfully. We next move on to our second question, which is whether these neural  
523 representations change when overt behaviour *is* affected, and therefore, whether we can use the  
524 neural activity as measured by MEG to predict behavioural errors before they occur. We used our  
525 method of error data analysis (Woolgar et al., 2019) to examine whether the patterns of information  
526 coding on miss trials differed from correct trials (see *Methods*). For these analyses we used only  
527 attended dots, as unattended dots do not have behavioural responses, and we matched the total  
528 number of trials in our implementation of correct and miss classification.

529

530 First, we evaluated the processing of the less relevant information - the *direction of approach*  
531 measure (Figure 5A). The results for *correct* trials provided information dynamics very similar to the  
532 attended condition in Figure 3A, except for higher overall decoding, which is explained by the

533 inclusion of the data from the whole experiment (15 blocks) rather than just the five early and late  
 534 blocks (note the number of trials is still matched to miss trials).

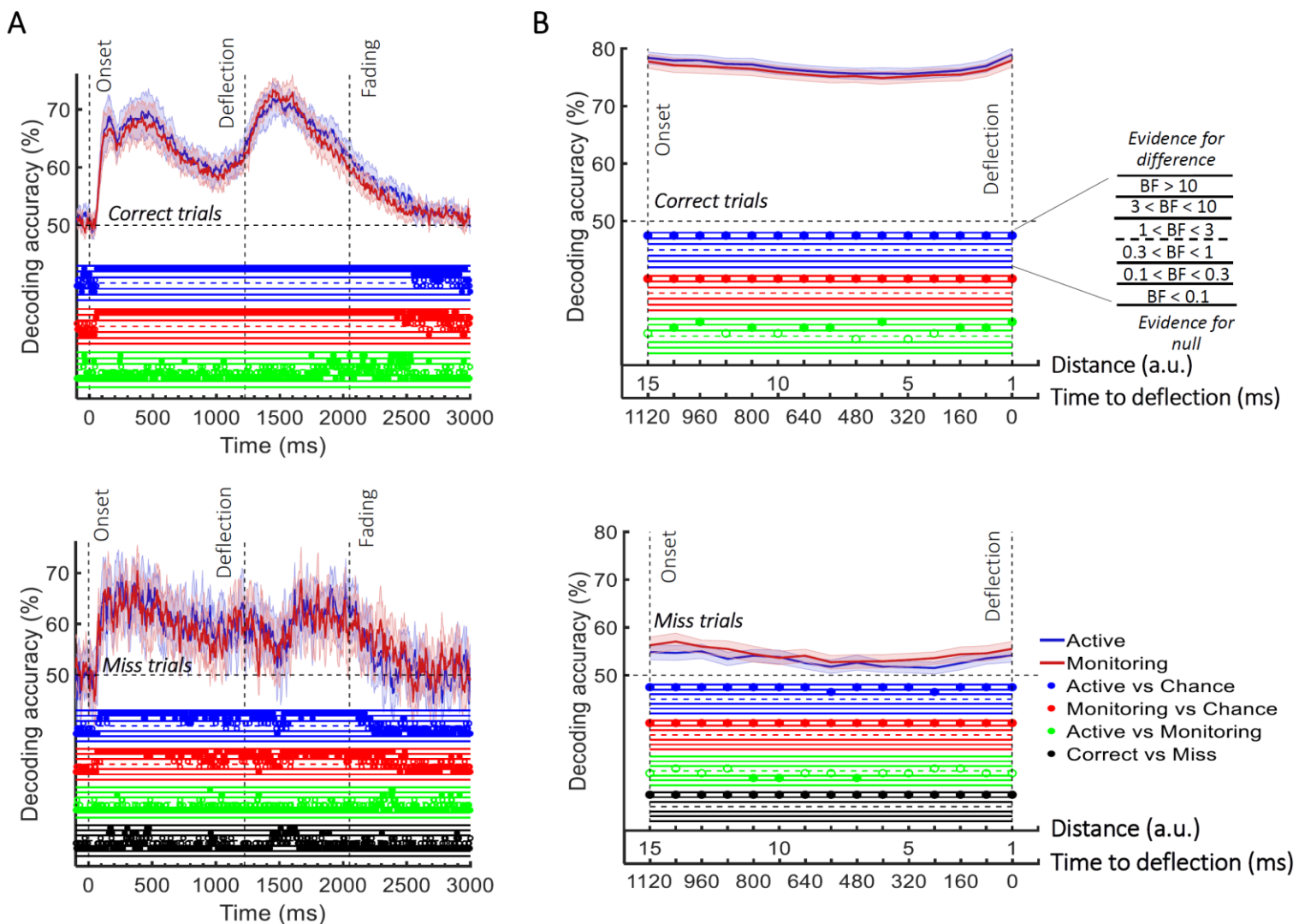


Figure 5. Decoding of information on *correct* vs. *miss* trials. (A) Decoding of *direction of approach* information (less task-relevant). (B) Decoding of *distance to object* information (most task-relevant). The horizontal dashed lines refer to chance-level decoding. Top panels: Decoding using *correct trials*; Bottom panels: Decoding using *miss trials*. In both top and bottom panels, the classifiers were trained on *correct trials* and tested on (left out) *correct* and all *miss trials*, respectively. Thick lines show the average across participants (shading 95% confidence intervals). Vertical dashed lines indicate critical events in the trial. Bayes Factors are shown in the bottom section of each graph: Filled circles show moderate/strong evidence for either hypothesis and empty circles indicate insufficient evidence. They show the results of Bayes factor analysis when evaluating the difference of the decoding values from chance for Active (blue) and Monitoring (red) conditions separately, the comparison of the two conditions (green) and the comparison of correct and miss trials (black). Note that for the comparison of correct and miss trials, Active and Monitoring conditions were averaged separately.

535

536 Active and Monitoring conditions did not show any time windows of sustained difference ( $BF < 0.3$ ).  
537 However, when the classifiers were tested on *miss* trials, from onset to deflection, the pattern of  
538 information dynamics were different, even though we had matched the number of trials.  
539 Specifically, while the level of information was comparable to *correct* trials with spurious instances  
540 (but no sustained time windows) of difference ( $BF > 3$  as indicated by black dots) before 500 ms,  
541 decoding traces were much noisier for *miss* trials with more variation across trials and between  
542 nearby time points (Figure 5A). Note that after the deflection, the visual signal is different for correct  
543 and miss trials, so the difference between their decoding curves ( $BF > 3$ ) is not meaningful. These  
544 results suggest a noisier processing of *direction of approach* information for the missed dots  
545 compared to correctly deflected dots.

546

547 We then repeated the same procedure on the processing of the most task-relevant *distance to*  
548 *object* information on *correct* vs. *miss* trials (Figure 5B). Although on *correct* trials, the distance  
549 information for both Active and Monitoring conditions was well above chance (77%;  $BF > 10$ ), for  
550 *miss* trials, the corresponding distance information was only just above chance (55%;  $BF > 10$  for all  
551 distances except one). The direct comparison revealed that distance information dropped  
552 considerably on *miss* trials compared to *correct* trials (Figure 5; Black dots;  $BF > 10$  across all  
553 distances; Active and Monitoring results were averaged for correct and miss trials separately before  
554 Bayes analyses). This is consistent with less representation of the crucial information about the  
555 distance from the object preceding a behavioural miss.

556

557 [Can we predict behavioural errors using neuroimaging?](#)

558 Finally, we asked whether we could use this information to predict the behavioural outcome of each  
559 trial. To do so, we developed a new method that classified trials based on their behavioural  
560 outcomes (correct vs. miss) by asking how well a set of classifiers, pre-trained on correct trials,

561 would classify the distance of the dot from the target (see *Methods*; Figure 6A). To achieve this, we  
562 used a second-level classifier which labelled a trial as correct or miss based on the average  
563 accumulated accuracies obtained for that dot at every distance from the first-level decoding  
564 classifiers which were trained on *correct* trials (Figure 6A and 6B; see *Methods*). If the accumulated  
565 accuracy for the given dot at the given distance was less than the average accuracy obtained from  
566 testing on the validation set minus a specific threshold (based on standard deviation), the testing dot  
567 (trial) was labelled as *correct*, otherwise *miss*. As Figure 6B shows, there was strong evidence ( $BF >$   
568 10) that decoding accuracy of distances was higher for *correct* than *miss* trials with the inclusion of  
569 more classifier accuracies as the dot approached from the corner of the screen towards the centre  
570 with a multiple of around 1.5 as threshold (Figure 6C). This clear separation of accumulated  
571 accuracies for *correct* vs. *miss* trials allowed us to predict with above-chance accuracy the  
572 behavioural outcome of the ongoing trial (Figure 6D). To find the optimal threshold for each  
573 participant, we evaluated the thresholds used for all other participants except for a single testing  
574 participant for whom we used the average of the best thresholds that led to highest prediction  
575 accuracy for other participants. This was  $\sim$ 1.5 standard deviation below the average accuracy on the  
576 other participants' validation (correct trial) sets (Figure 6C).

577

578 The prediction accuracy of behavioural outcome was above chance level (68% vs. 50%;  $BF > 10$ ) even  
579 when the dot had only been on the screen for 80ms, which corresponds to our furthest distance #15  
580 (1200ms prior to deflection point; Figure 6D). The accuracy increased to 85% as the dot approached  
581 the centre of the screen, with  $\sim$ 80% accuracy with still 800 ms to go before required response.  
582 Importantly, the prediction algorithm showed generalisable results across participants; the threshold  
583 for decision obtained from the other participants could predict the accuracy of an independent  
584 participant's behaviour using only their neural data.

585

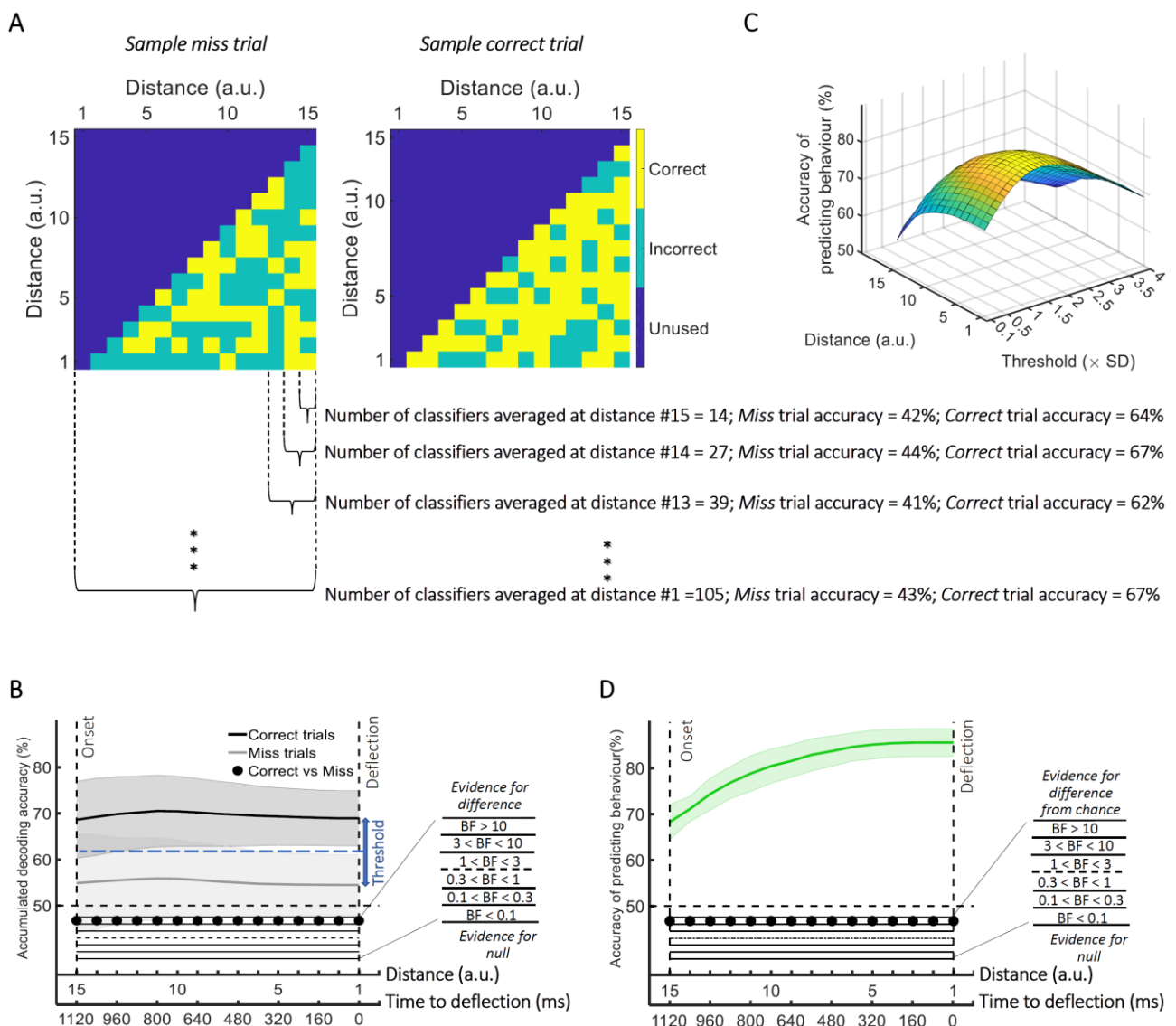


**Figure 6. Prediction of behavioural outcome (*correct* vs. *miss*) trial-by-trial using decoding of *distance to object* information.** (A) Sample classifiers' accuracies (correct or incorrect classification of current distance as indicated by colors) for a *miss* (left panel; average accuracy  $\approx 43\%$  when the dot reached the deflection point) and a *correct* trial (right panel; average accuracy  $\approx 67\%$  at the deflection point). The classifiers were trained on the data from *correct* trials and tested on the data from *correct* and *miss* trials. For the *miss* trials, around half the classifiers classified the dot's distance incorrectly by the time it reached the deflection point. (B) Accumulation of classifiers' accuracies over decreasing dot distances/time to deflection. This shows stronger information coding of the crucial *distance to object* information on the *correct* trials over *miss* trials. A variable threshold used in (C) is shown as a blue dashed line. (C) Prediction of behavioural outcome as a function of threshold and distance using a second-level behavioural outcome classification. Results show highest prediction accuracies on the participant set at around the threshold of 1.5 (see *Methods*), increasing at closer distances. (D) Accuracy of predicting behavioural outcome for the left-out participant using the threshold obtained from all the other participants as function of distance/time from the deflection point. Results showed successful ( $\approx 70\%$ ) prediction of behavioural outcome of the trial as early as 80 ms after stimulus appearance. Thick lines and shading refer to average and one standard deviation around the mean across participants, respectively. Bayes Factors are shown in the bottom section of each graph: Filled circles show moderate/strong evidence for either hypothesis and empty circles indicate insufficient evidence (black dots under B and D).

587 Please note that the results presented so far were from *correct* and *miss* trials and we excluded  
588 early, late and wrong-colour *false alarms* to be more specific about the error type. However, the  
589 false alarm results (collapsed across all three types of false alarms) were very similar (Supplementary  
590 Figure 2) to those of the missed trials (Figure 5): noisy information about the *direction of approach*  
591 and at-chance information about the *distance to object*. This may suggest that both miss and false  
592 alarm trials are caused by a similar impaired processing of information, or at least captured similarly  
593 by our decoding methods. The average number of miss trials was 58.17 ( $\pm 21.63$  SD) and false alarm  
594 trials was 65.94 ( $\pm 21.13$  SD; out of 1920 trials).

595

#### 596 [Can we decode direction and distance information from eye-tracking data?](#)

597 To see whether we could decode information about the dot motion using only the eye-tracking data,  
598 we repeated the same error data analysis as above, but this time using the 2-dimensional signals  
599 (i.e., corresponding to the x-y coordinates of the gaze location) provided by the eye-tracker (Görgen  
600 et al., 2018). The decoding of *direction of approach* from *correct* trials showed above-chance  
601 information (Supplementary Figure 3A) starting from 455 and 460 ms post-stimulus onset for the  
602 Active and Monitoring conditions ( $BF > 10$ ), respectively. The information on *miss* trials was noisier  
603 but showed a similar pattern. The correct and miss trials only showed moderate evidence ( $3 < BF <$   
604 10) for difference in the span from 310 ms to 490 ms. This suggests that participants moved their  
605 eyes differently for the dots approaching from opposite directions, which is not unexpected (and  
606 observed in the eye-tracking fixation points data). Although the dynamics of this decoding over time  
607 is different to the neural decoding, in line with visually evoked information decoding studies  
608 (VanRullen, 2007; Karimi-Rouzbhani et al., 2017), the eye-movement data do hold enough  
609 information to decode the *direction of approach*.

610

611 In contrast, for the crucial *distance to object* measure, although the eye-tracking data showed  
612 above-chance values at a few distances ( $BF > 10$ ; Supplementary Figure 3B), most were very close to  
613 chance and much lower than those obtained from the neural data (cf. Figure 5B;  $BF > 10$  for the  
614 difference between decoding of neural vs eyetracking data for correct trials; indicated by black dots  
615 in Supplementary Figure 3A). Only for the decoding for *miss* vs. *correct* trials was there any evidence  
616 (moderate) for similarity between neural and eyetracking data ( $0.1 < BF < 0.3$ ; black dots;  
617 Supplementary Figure 3B). Note that *distance to object* data collapses across identical distances from  
618 the left and right sides of the screen, which avoids the potential confound of eye-movements data  
619 driving the classifier for this crucial distance measure.

620

## 621 Discussion

622 This study developed new methods to gain insights into how attention, the frequency of target  
623 events, and the time doing a task affect the representation of task information in the brain. Our new  
624 multiple object monitoring (MOM) task evoked reliable vigilance decrements in both accuracy and  
625 reaction time in a situation that more closely resembles real-life modern tasks than classic vigilance  
626 tasks. By using the sensitive analysis method of MVPA, we were able to test information coding  
627 across task conditions to evaluate the neural correlates of vigilance decrements. We also developed  
628 a novel informational brain connectivity method, which allowed evaluation of the correlation  
629 between information coding across peri-occipital and peri-frontal areas in different task conditions,  
630 to investigate the brain connectivity under different levels of attention, target frequency and the  
631 time on the task. Finally, we utilised our recent error data analysis to predict forthcoming  
632 behavioural misses with high accuracy. In the following sections, we explain each of the four  
633 contributions in detail and compare them with relevant literature.

634

635 First, the MOM task includes key features of real-world monitoring situations that are not usually  
636 part of other vigilance tasks (e.g., Mackworth, 1948; Temple, 2000; Rosvold et al., 1956; Rosenberg  
637 et al., 2013), and the results show clear evidence of vigilance decrements. Behavioural performance,  
638 measure with both reaction time and accuracy, deteriorated over time in monitoring (infrequent  
639 target) relative to active (frequent target) conditions. These vigilance decrements demonstrate that  
640 the MOM task can be used to explore vigilance in situations more closely resembling modern  
641 environments, namely involving moving stimuli and selection of relevant from irrelevant  
642 information, giving a useful tool for future research.

643

644 Second, the high sensitivity of MVPA to extract information from neural signals allowed us to  
645 investigate the temporal variations in processing as the experiment progressed. The manipulation of  
646 attention showed a strong overall effect with enhanced representation of both the less important  
647 *direction of approach* and the most task-relevant *distance to object* information for cued dots,  
648 regardless of how frequent the targets were (Figure 3). The improved representation of information  
649 under attention extends previous findings from us and others (Woolgar et al., 2015b; Goddard et al.,  
650 2019; Nastase et al., 2017) to moving displays, in which the participants monitor multiple objects  
651 simultaneously.

652

653 The manipulation of target frequency showed that when participants only had to respond  
654 infrequently, modelling real-life monitoring situations, the neural coding of crucial information about  
655 the task dropped, correlating with the decrease in behavioural performance (i.e., vigilance effects in  
656 both accuracy and RT; Figure 2). This suggests that when people monitor for rare targets, they  
657 process or encode the relevant information less effectively as the time passes relative to conditions  
658 in which they are actively engaged in completing the task. Several previous studies have examined  
659 the neural correlates of vigilance decrements using univariate analyses (for a review see Langner et

660 al. (2013)). However, univariate analyses fail to capture widespread but subtle differences of  
661 patterns between conditions across distant brain networks. One recent study utilized the sensitivity  
662 of MVPA to extract task-relevant and task-irrelevant information under sustained attention (Megan  
663 et al., 2015). In this case, however, the aspects of information were similar in identity (i.e. high-level  
664 visual categories of face and scenes) and switched their attentional role (i.e. attended vs.  
665 unattended) across the experiment, which makes it difficult to see whether (if at all) vigilance  
666 decrements would differentially affect encoding of different aspects of information depending on  
667 their relevance to the task. To address this issue, here we not only switched the task-relevance of  
668 information across the experiment to replicate the attentional effect of that study (i.e. cued/un-cued  
669 dots), but we also studied two aspects of the dot motion information that varied in importance for  
670 carrying out the task (i.e., *direction of approach* and *distance to object*) with unchanging roles across  
671 the experiment. While switching between dot colours showed the effect of attention, with greater  
672 representation of the cued dots over uncued dots, the relevance of the *direction of approach* and  
673 the *distance to object* did not vary. The less relevant direction information was unaffected by target  
674 frequency, whereas the coding of the critical task-relevant distance information correlated with the  
675 decrease in behavioural performance over time. This is relevant to theories of vigilance, by  
676 demonstrating that the task-relevance of information might be a major factor in whether vigilance  
677 decrements occur.

678

679 It is important to note that previous studies have tried other physiological/behavioural measures to  
680 determine participants' vigilance or alertness, such as pupil size (Yoss et al., 1970), response time  
681 variability (Rosenberg et al., 2013), blood pressure and thermal energy (Lohani et al., 2019) or even  
682 body temperature (Molina et al., 2019). We used highly-sensitive analysis of neuroimaging data so  
683 that we could address two questions that could not be answered using these more general vigilance  
684 measures. Our approach allowed us to test for changes in the way information is processed in the

685 brain, particularly testing for differences in the impact of monitoring on the relevance of the  
686 information, rather than whether the participants were vigilant and alert in general. Moreover, we  
687 could also investigate how relevant and less relevant information was affected by the target  
688 frequency and time on the task, which could explain the behavioural vigilance decrement observed  
689 in many previous studies (e.g., Dehais et al., 2019; Wolfe et al., 2005; Wolfe et al., 2007; Kamzanova  
690 et al., 2014; Ishibashi et al., 2012). We tested our methods also on the eye-tracking data and found  
691 that the critical task-relevant information change under monitoring conditions could not be  
692 replicated based on eye-movements, demonstrating the benefit of the neural approach.

693

694 Third, our information-based brain connectivity method showed weaker connectivity between the  
695 peri-frontal attentional network and the peri-occipital visual areas of the brain in the unattended  
696 and monitoring conditions (Figure 4), where participants encountered fewer targets relative to the  
697 other conditions. We also observed less connectivity between the same areas on *miss* vs. *correct*  
698 trials, which might explain the behavioural outcome of the trials. Most previous neuroimaging  
699 studies have used univariate brain connectivity analyses, which are prone to missing existing  
700 functional connectivity across areas when encountering low-amplitude activity on individual sensors  
701 (Anzellotti & Coutanche, 2018; Basti et al., 2020). The method we used here evaluated the  
702 correlation between representational dissimilarity matrices, which has provided high-dimensional  
703 information about *distance to object*, obtained from multiple sensors across the brain areas. This  
704 makes the analysis more sensitive to capturing subtle connectivity and also aligns with a major  
705 recent shift in literature from univariate to multivariate informational connectivity analyses  
706 (Goddard et al., 2016; Goddard et al., 2019; Karimi-Rouzbahani et al., 2019; Karimi-Rouzbahani,  
707 2017; Anzellotti & Coutanche, 2018; Basti et al., 2020).

708

709 Fourth, building upon our recently-developed method of error analysis (Woolgar et al., 2019), we  
710 were able to predict forthcoming behavioural misses before the response was given. This method  
711 only used *correct* trials for training, which makes its implementation plausible for real-world  
712 situations since we usually have plenty of correct trials and only few miss trials (i.e., cases when the  
713 railway controller diverts the trains correctly vs. misses and a collision happens). In our study, the  
714 method showed a large decline in the crucial task-relevant (i.e., *distance to object*) information  
715 decoding on *miss* vs. *correct* trials but less decline in the less task-relevant information (i.e., *direction*  
716 *of approach*). A complementary analysis allowed the prediction of behaviourally missed trials as  
717 soon as the stimulus appeared on the screen (after ~80 ms), which was ~1200 ms before the time of  
718 response. This method was generalisable across participants, with the decision threshold for trial  
719 classification other participants' data successful in predicting errors for a left-out participant. A  
720 number of previous studies have shown that behavioural performance could be correlated with  
721 aspects of brain activity even before the stimulus onset (Eichele et al., 2008; Weissman et al., 2006;  
722 Sadaghiani et al., 2015). This can be crucial for many high-risk environments, including semi-  
723 autonomous car driving and railway control. Those studies have explained the behavioural errors by  
724 implicit measures such as less deactivation of the default-mode network, reduced stimulus-evoked  
725 sensory activity (Weissman et al., 2006; Eichele et al., 2008) and even the connectivity between  
726 sensory and vigilance-related/default-mode brain areas (Sadaghiani et al., 2015). It would be  
727 informative, however, if they could show how (if at all) the processing of task-relevant information is  
728 disrupted in the brain and how this might lead to behavioural errors. To serve an applied purpose, it  
729 would be ideal if there was a procedure to use those neural signatures to predict behavioural  
730 outcomes. Only two previous studies have approached this goal. Sadaghiani et al. (2015) and Dehais  
731 et al. (2019) reported maximum prediction accuracies of 63% and 72% (with adjusted chance levels  
732 of 55% and 59%, respectively), far lower than what we have obtained here (up to 85% with a chance  
733 level of 50%), suggesting our method accesses more relevant neural signatures of vigilance  
734 decrements, or is more sensitive in discriminating these. The successful prediction of an error from

735 neural data more than a second in advance of the impending response provides a promising avenue  
736 for detecting lapses of attention before any consequences occur.

737

738 Current explanations for vigilance effects generally fall into two categories: mind-wandering and  
739 cognitive overload. In the first, the low cognitive demands of monitoring tasks result in mind-  
740 wandering and then, when a response is required, there are insufficient resources dedicated to the  
741 task (e.g., malleable attention theory (Manly et al., 1999; Smallwood et al., 2006; Young et al.,  
742 2002)). In the second, the demands of sustaining attention depletes cognitive resources over time  
743 leading to insufficient resources and increased errors in later stages of the task (e.g., Helton et al.,  
744 2008; Helton et al., 2011; Warm et al., 2008). There are several previous observations of decreased  
745 functional connectivity during mind wandering (Chou et al., 2017; Kucyi et al., 2018; van Son et al.,  
746 2019), which our informational connectivity results broadly replicate. For example, Chou et al.  
747 (2017) reported a decrease in functional connectivity between visual and sensorimotor and in turn  
748 to frontal brain areas in later stages of a resting-state mind-wandering fMRI study in which  
749 participants were instructed to draw their mind to specific but broad sets of thoughts. In another  
750 study, using EEG-fMRI, von Son et al. (2019) found reduced functional connectivity between the  
751 dorsolateral PFC, dorsal anterior cingulate cortex (ACC), and posterior parietal regions, namely the  
752 “executive control network”, when participants counted and reported their number of inhales and  
753 episodes of mind wandering. Our finding of a decrease in higher order cognitive (peri-frontal) and  
754 sensory (peri-occipital) areas in later (compared with early) stages of the experiment is broadly  
755 consistent with these findings, but we are unable to distinguish whether this is due to mind  
756 wandering or the depletion of cognitive resources, as in our task either is a plausible explanation for  
757 the effect.

758

759 The overall goal of this study was to understand how neural information processing of dynamic  
760 displays were affected by attention and target frequency, and whether reliable changes in behaviour  
761 over time could be predicted on the basis of neural patterns. We observed that the neural  
762 representation of critically relevant information in the brain decreases over time, especially when  
763 targets are infrequent. This neural representation was particularly poor on trials where participants  
764 missed the target. We used this observation to predict behavioural outcome of individual trials, and  
765 showed that we could accurately predict behavioural outcome more than a second before action  
766 was needed. These results provide new insights about how vigilance decrements impact information  
767 coding in the brain and propose an avenue for predicting behavioural errors using novel  
768 neuroimaging analysis techniques.

769

## 770 Acknowledgments

771 This work was funded by an Australian Research Council (ARC) Discovery Project grant to A.N.R and  
772 A.W. (DP170101780). A.W. was supported by an ARC Future Fellowship (FT170100105) and MRC  
773 intramural funding SUAG/052/G101400. We thank Denise Moerel, Mark Wiggins, Jeremy Wolfe and  
774 William Helton for contributions to an earlier design of the MOM task.

775

## 776 References

777 Adler, C. M., Sax, K. W., Holland, S. K., Schmithorst, V., Rosenberg, L., & Strakowski, S. M. (2001). Changes  
778 in neuronal activation with increasing attention demand in healthy volunteers: an fMRI study. *Synapse*, 42(4),  
779 266-272.

780 Alnaes, D., Kaufmann, T., Richard, G., Duff, E. P., Snee, M. H., Endestad, T., ... & Westlye, L. T. (2015).  
781 Attentional load modulates large-scale functional brain connectivity beyond the core attention networks.  
782 *Neuroimage*, 109, 260-272.

783 Anzellotti, S., & Coutanche, M. N. (2018). Beyond functional connectivity: investigating networks of  
784 multivariate representations. *Trends in cognitive sciences*, 22(3), 258-269.

785 Basti, A., Nili, H., Hauk, O., Marzetti, L., & Henson, R. (2020, February 11). Multivariate connectivity: a  
786 conceptual and mathematical review. <https://doi.org/10.31219/osf.io/2q9v4>

787 Baillet, S. (2017). Magnetoencephalography for brain electrophysiology and imaging. *Nature neuroscience*,  
788 20(3), 327-339.

789 Benedict, R. H., Shucard, D. W., Maria, M. P. S., Shucard, J. L., Abara, J. P., Coad, M. L., ... & Lockwood, A.  
790 (2002). Covert auditory attention generates activation in the rostral/dorsal anterior cingulate cortex. *Journal of*  
791 *Cognitive Neuroscience*, 14(4), 637-645.

792 Brainard, D. H. (1997). The psychophysics toolbox. *Spatial vision*, 10(4), 433-436.

793 Chou, Y. H., Sundman, M., Whitson, H. E., Gaur, P., Chu, M. L., Weingarten, C. P., ... & Diaz, M. T. (2017).  
794 Maintenance and representation of mind wandering during Resting-State fMRI. *Scientific reports*, 7, 40722.

795 Coull, J. T., Frith, C. D., Frackowiak, R. S. J., & Grasby, P. M. (1996). A fronto-parietal network for rapid  
796 visual information processing: a PET study of sustained attention and working memory. *Neuropsychologia*,  
797 34(11), 1085-1095.

798 Dehais, F., Roy, R. N., & Scannella, S. (2019). Inattentional deafness to auditory alarms: Inter-individual  
799 differences, electrophysiological signature and single trial classification. *Behavioural brain research*, 360, 51-59.

800 Dienes, Z. (2014). Using Bayes to get the most out of non-significant results. *Frontiers in psychology*, 5, 781.

801 Duncan, J. (2010). The multiple-demand (MD) system of the primate brain: mental programs for intelligent  
802 behaviour. *Trends in cognitive sciences*, 14(4), 172-179.

803 Duncan, J., & Owen, A. M. (2000). Common regions of the human frontal lobe recruited by diverse cognitive  
804 demands. *Trends in neurosciences*, 23(10), 475-483.

805 Eichele, H., Juvodden, H., Ullsperger, M., & Eichele, T. (2010). Mal-adaptation of event-related EEG responses  
806 preceding performance errors. *Frontiers in human neuroscience*, 4, 65.

807 Eichele, T., Debener, S., Calhoun, V. D., Specht, K., Engel, A. K., Hugdahl, K., ... & Ullsperger, M. (2008).  
808 Prediction of human errors by maladaptive changes in event-related brain networks. *Proceedings of the National  
809 Academy of Sciences*, 105(16), 6173-6178.

810 Fedorenko, E., Duncan, J., & Kanwisher, N. (2013). Broad domain generality in focal regions of frontal and  
811 parietal cortex. *Proceedings of the National Academy of Sciences*, 110(41), 16616-16621.

812 Gilbert, S. J., Simons, J. S., Frith, C. D., & Burgess, P. W. (2006). Performance-related activity in medial rostral  
813 prefrontal cortex (area 10) during low-demand tasks. *Journal of Experimental Psychology: Human Perception  
814 and Performance*, 32(1), 45.

815 Goddard, E., Carlson, T. A., & Woolgar, A. (2019). Spatial and feature-selective attention have distinct effects  
816 on population-level tuning. *bioRxiv*, 530352.

817 Goddard, E., Carlson, T. A., Dermody, N., & Woolgar, A. (2016). Representational dynamics of object  
818 recognition: Feedforward and feedback information flows. *Neuroimage*, 128, 385-397.

819 Görzen, K., Hebart, M. N., Allefeld, C., & Haynes, J. D. (2018). The same analysis approach: Practical  
820 protection against the pitfalls of novel neuroimaging analysis methods. *Neuroimage*, 180, 19-30.

821 Greicius, M. D., Krasnow, B., Reiss, A. L., & Menon, V. (2003). Functional connectivity in the resting brain: a  
822 network analysis of the default mode hypothesis. *Proceedings of the National Academy of Sciences*, 100(1),  
823 253-258.

824 Greicius, M. D., Supekar, K., Menon, V., & Dougherty, R. F. (2009). Resting-state functional connectivity  
825 reflects structural connectivity in the default mode network. *Cerebral cortex*, 19(1), 72-78.

826 Grootswagers, T., Wardle, S. G., & Carlson, T. A. (2017). Decoding dynamic brain patterns from evoked  
827 responses: A tutorial on multivariate pattern analysis applied to time series neuroimaging data. *Journal of*  
828 *cognitive neuroscience*, 29(4), 677-697

829 Helton, W. S., & Russell, P. N. (2011). Feature absence–presence and two theories of lapses of sustained  
830 attention. *Psychological research*, 75(5), 384-392.

831 Helton, W. S., & Warm, J. S. (2008). Signal salience and the mindlessness theory of vigilance. *Acta  
832 psychologica*, 129(1), 18-25.

833 Indovina, I., & Macaluso, E. (2004). Occipital–parietal interactions during shifts of exogenous visuospatial  
834 attention: trial-dependent changes of effective connectivity. *Magnetic resonance imaging*, 22(10), 1477-1486.

835 Ishibashi, K., Kita, S., & Wolfe, J. M. (2012). The effects of local prevalence and explicit expectations on  
836 search termination times. *Attention, Perception, & Psychophysics*, 74(1), 115-123.

837 Jeffreys, H. (1961). *Theory of probability* (3rd ed.). New York: Oxford University Press.

838 Johannsen, P., Jakobsen, J., Bruhn, P., Hansen, S. B., Gee, A., Stødkilde-Jørgensen, H., & Gjedde, A. (1997).  
839 Cortical sites of sustained and divided attention in normal elderly humans. *Neuroimage*, 6(3), 145-155.

840 Kamzanova, A. T., Kustubayeva, A. M., & Matthews, G. (2014). Use of EEG workload indices for diagnostic  
841 monitoring of vigilance decrement. *Human factors*, 56(6), 1136-1149.

842 Karimi-Rouzbahani, H. (2018). Three-stage processing of category and variation information by entangled  
843 interactive mechanisms of peri-occipital and peri-frontal cortices. *Scientific reports*, 8(1), 1-22.

844 Karimi-Rouzbahani, H., Bagheri, N., & Ebrahimpour, R. (2017). Hard-wired feed-forward visual mechanisms  
845 of the brain compensate for affine variations in object recognition. *Neuroscience*, 349, 48-63.

846 Karimi-Rouzbahani, H., Vahab, E., Ebrahimpour, R., & Menhaj, M. B. (2019). Spatiotemporal analysis of  
847 category and target-related information processing in the brain during object detection. *Behavioural brain  
848 research*, 362, 224-239.

849 Kleiner, M., Brainard, D., & Pelli, D. (2007). What's new in Psychtoolbox-3?

850 Kriegeskorte, N., Mur, M., & Bandettini, P. A. (2008). Representational similarity analysis-connecting the  
851 branches of systems neuroscience. *Frontiers in systems neuroscience*, 2, 4.

852 Kucyi, A. (2018). Just a thought: How mind-wandering is represented in dynamic brain connectivity.  
853 *Neuroimage*, 180, 505-514.

854 Langner, R., & Eickhoff, S. B. (2013). Sustaining attention to simple tasks: a meta-analytic review of the neural  
855 mechanisms of vigilant attention. *Psychological bulletin*, 139(4), 870.

856 Lee, M., & Wagenmakers, E. J. (2005). Bayesian statistical inference in psychology: comment on Trafimow  
857 (2003). *Psychological Review*, 112, 662–668.

858 Lohani, M., Payne, B. R., & Strayer, D. L. (2019). A review of psychophysiological measures to assess  
859 cognitive states in real-world driving. *Frontiers in human neuroscience*, 13.

860 Mackworth, N. H. (1948). The breakdown of vigilance during prolonged visual search. *Quarterly Journal of  
861 Experimental Psychology*, 1(1), 6-21.

862 Manly, T., Robertson, I. H., Galloway, M., & Hawkins, K. (1999). The absent mind: further investigations of  
863 sustained attention to response. *Neuropsychologia*, 37(6), 661-670.

864 Mazaheri, A., Nieuwenhuis, I. L., Van Dijk, H., & Jensen, O. (2009). Prestimulus alpha and mu activity predicts  
865 failure to inhibit motor responses. *Human brain mapping*, 30(6), 1791-1800.

866 Megan, T. D., Cohen, J. D., Lee, R. F., Norman, K. A., & Turk-Browne, N. B. (2015). Closed-loop training of  
867 attention with real-time brain imaging. *Nature neuroscience*, 18(3), 470.

868 Molina, E., Sanabria, D., Jung, T. P., & Correa, A. (2019). Electroencephalographic and peripheral temperature  
869 dynamics during a prolonged psychomotor vigilance task. *Accident Analysis & Prevention*, 126, 198-208.

870 Nastase, S. A., Connolly, A. C., Oosterhof, N. N., Halchenko, Y. O., Guntupalli, J. S., Visconti di Oleggio  
871 Castello, M., ... & Haxby, J. V. (2017). Attention selectively reshapes the geometry of distributed semantic  
872 representation. *Cerebral Cortex*, 27(8), 4277-4291.

873 O'Connell, R. G., Dockree, P. M., Robertson, I. H., Bellgrove, M. A., Foxe, J. J., & Kelly, S. P. (2009).  
874 Uncovering the neural signature of lapsing attention: electrophysiological signals predict errors up to 20 s before  
875 they occur. *Journal of Neuroscience*, 29(26), 8604-8611.

876 Ortuno, F., Ojeda, N., Arbizu, J., Lopez, P., Marti-Climent, J. M., Penuelas, I., & Cervera, S. (2002). Sustained  
877 attention in a counting task: normal performance and functional neuroanatomy. *Neuroimage*, 17(1), 411-420.

878 Périn, B., Godefroy, O., Fall, S., & De Marco, G. (2010). Alertness in young healthy subjects: an fMRI study of  
879 brain region interactivity enhanced by a warning signal. *Brain and cognition*, 72(2), 271-281.

880 Raichle, M. E. (2015). The brain's default mode network. *Annual review of neuroscience*, 38, 433-447.

881 Rich, A. N., Kunar, M. A., Van Wert, M. J., Hidalgo-Sotelo, B., Horowitz, T. S., & Wolfe, J. M. (2008). Why  
882 do we miss rare targets? Exploring the boundaries of the low prevalence effect. *Journal of Vision*, 8(15), 15-15.

883 Rosenberg, M., Noonan, S., DeGutis, J., & Esterman, M. (2013). Sustaining visual attention in the face of  
884 distraction: a novel gradual-onset continuous performance task. *Attention, Perception, & Psychophysics*, 75(3),  
885 426-439.

886 Rosvold, H. E., Mirsky, A. F., Sarason, I., Bransome Jr, E. D., & Beck, L. H. (1956). A continuous performance  
887 test of brain damage. *Journal of consulting psychology*, 20(5), 343.

888 Rouder, J. N., Morey, R. D., Speckman, P. L., & Province, J. M. (2012). Default Bayes factors for ANOVA  
889 designs. *Journal of Mathematical Psychology*, 56(5), 356-374.

890 Sadaghiani, S., Poline, J. B., Kleinschmidt, A., & D'Esposito, M. (2015). Ongoing dynamics in large-scale  
891 functional connectivity predict perception. *Proceedings of the National Academy of Sciences*, 112(27), 8463-  
892 8468.

893 Schnell, K., Heekeren, K., Schnitker, R., Daumann, J., Weber, J., Heßelmann, V., ... & Gouzoulis-Mayfrank, E.  
894 (2007). An fMRI approach to particularize the frontoparietal network for visuomotor action monitoring:  
895 detection of incongruence between test subjects' actions and resulting perceptions. *Neuroimage*, 34(1), 332-341.

896 Smallwood, J., & Schooler, J. W. (2006). The restless mind. *Psychological bulletin*, 132(6), 946.

897 Sturm, W., De Simone, A., Krause, B. J., Specht, K., Hesselmann, V., Radermacher, I., ... & Willmes, K.  
898 (1999). Functional anatomy of intrinsic alertness: evidence for a fronto-parietal-thalamic-brainstem network in  
899 the right hemisphere. *Neuropsychologia*, 37(7), 797-805.

900 Tana, M. G., Montin, E., Cerutti, S., & Bianchi, A. M. (2010). Exploring cortical attentional system by using  
901 fMRI during a Continuous Performance Test. *Computational intelligence and neuroscience*, 2010.

902 Temple, J. G., Warm, J. S., Dember, W. N., Jones, K. S., LaGrange, C. M., & Matthews, G. (2000). The effects  
903 of signal salience and caffeine on performance, workload, and stress in an abbreviated vigilance task. *Human  
904 factors*, 42(2), 183-194.

905 Thakral, P. P., & Slotnick, S. D. (2009). The role of parietal cortex during sustained visual spatial attention.  
906 *Brain Research*, 1302, 157-166.

907 van Son, D., de Rover, M., De Blasio, F. M., van der Does, W., Barry, R. J., & Putman, P. (2019).  
908 Electroencephalography theta/beta ratio covaries with mind wandering and functional connectivity in the  
909 executive control network. *Annals of the New York Academy of Sciences*, 1452(1), 52.

910 VanRullen, R. (2007). The power of the feed-forward sweep. *Advances in Cognitive Psychology*, 3(1-2), 167.

911 Warm, J. S., Parasuraman, R., & Matthews, G. (2008). Vigilance requires hard mental work and is stressful.  
912 *Human factors*, 50(3), 433-441.

913 Weissman, D. H., Roberts, K. C., Visscher, K. M., & Woldorff, M. G. (2006). The neural bases of momentary  
914 lapses in attention. *Nature neuroscience*, 9(7), 971-978.

915 Wingen, M., Kuypers, K. P., van de Ven, V., Formisano, E., & Ramaekers, J. G. (2008). Sustained attention and  
916 serotonin: a pharmaco-fMRI study. *Human Psychopharmacology: Clinical and Experimental*, 23(3), 221-230.

917 Wolfe, J. M., Horowitz, T. S., & Kenner, N. M. (2005). Rare items often missed in visual searches. *Nature*,  
918 435(7041), 439-440.

919 Wolfe, J. M., Horowitz, T. S., Van Wert, M. J., Kenner, N. M., Place, S. S., & Kibbi, N. (2007). Low target  
920 prevalence is a stubborn source of errors in visual search tasks. *Journal of experimental psychology: General*,  
921 136(4), 623.

922 Woolgar, A., Afshar, S., Williams, M. A., & Rich, A. N. (2015a). Flexible coding of task rules in frontoparietal  
923 cortex: an adaptive system for flexible cognitive control. *Journal of cognitive neuroscience*, 27(10), 1895-1911.

924 Woolgar, A., Dermody, N., Afshar, S., Williams, M. A., & Rich, A. N. (2019). Meaningful patterns of  
925 information in the brain revealed through analysis of errors. *bioRxiv*, 673681.

926 Woolgar, A., Hampshire, A., Thompson, R., & Duncan, J. (2011). Adaptive coding of task-relevant information  
927 in human frontoparietal cortex. *Journal of Neuroscience*, 31(41), 14592-14599.

928 Woolgar, A., Williams, M. A., & Rich, A. N. (2015b). Attention enhances multi-voxel representation of novel  
929 objects in frontal, parietal and visual cortices. *Neuroimage*, 109, 429-437.

930 Yoss, R. E., Moyer, N. J., & Hollenhorst, R. W. (1970). Pupil size and spontaneous pupillary waves associated  
931 with alertness, drowsiness, and sleep. *Neurology*, 20(6), 545-545.

932 Young, M. S., & Stanton, N. A. (2002). Malleable attentional resources theory: a new explanation for the effects  
933 of mental underload on performance. *Human factors*, 44(3), 365-375.

934 Zellner, A., & Siow, A. (1980). Posterior odds ratios for selected regression hypotheses. In J.M. Bernardo, M.H.  
935 DeGroot, D.V. Lindley, A.F.M. Smith (Eds.), *Bayesian Statistics: proceedings of the first international meeting*  
936 held in Valencia (Spain) (585-603). University of Valencia.

937

938

939

940

941

942

943

944

945

946

947

948

949

950

951

952

953

954

955

956

957

958

959

960

961

962

963 **Supplementary Material**

964 **Supplementary figure 1 shows the same decoding results as presented in Figure 3 but**  
965 **evaluated against chance-level decoding (50%).**

966 Our first analysis was to verify that our analyses could decode the important aspects of the display,  
967 relative to chance, given the overlapping moving stimuli. Here, we give the detailed results of this  
968 analysis.

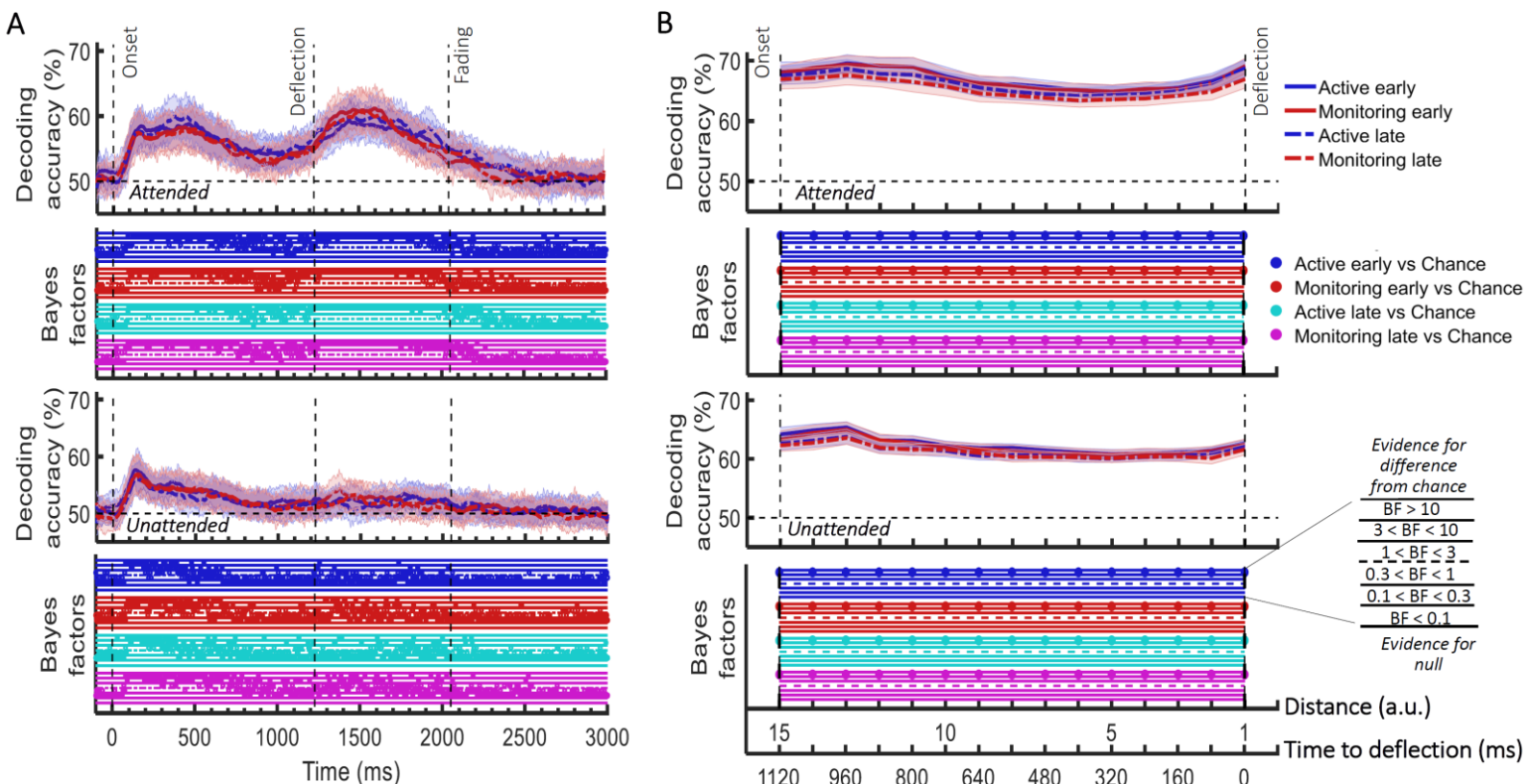
969  
970 We started with the information about the *direction of approach* (top left or bottom right of screen)  
971 which is a strong visual signal but not critical to the task decision. From 95 ms post-stimulus onset  
972 onwards, this visual information could be decoded from the MEG signal for all combinations of the  
973 factors: Attended and Unattended dots, both Target Frequency conditions (Active, Monitoring), and  
974 both our Time on Task durations (Early - first 5 blocks; Late - last 5 blocks; all BF > 10, different from  
975 chance).

976  
977 All conditions were decodable above chance until at least 385 ms post-stimulus onset (BF > 3;  
978 Supplementary Figure 1A), which was when the dots came closer to the centre, losing their visual  
979 difference. There was a rapid increase in information about the *direction of approach* between 50  
980 ms to 150 ms post-stimulus onset, consistent with an initial forward sweep of visual information  
981 processing (VanRullen, 2007; Karimi-Rouzbahani et al., 2017; Karimi-Rouzbahani et al., 2019). For  
982 attended dots only (but regardless of the Target Frequency or Time on Task), the information then  
983 increased again before the deflection time, and remained different from chance until 1915 ms post-  
984 stimulus onset, which is just before the dot faded (Supplementary Figure 1A). The second rise of  
985 decoding, which was more pronounced for the attended dots, could reflect the increasing relevance  
986 to the task as the dot approached the crucial deflection point, but it could also be due to higher  
987 visual acuity in foveal compared to peripheral areas of the visual field. The decoding peak observed

988 after the deflection point for the attended dots, was most probably caused by the large visual  
989 difference between the deflection trajectories for the dots approaching from the left vs. right side of  
990 the screen (see the deflection trajectories in Figure 1A).

991  
992 The most task-relevant feature of the motion is the distance between the moving dot and the  
993 central object, with the deflection point of the trajectories being the key decision point. We  
994 therefore tested for decoding of distance information (*distance to object*, see *Methods*). There was a  
995 brief increase in decoding of *distance to object* for attended dots across the other factors (Target  
996 Frequency and Time on Task) between the 15<sup>th</sup> and 10<sup>th</sup> distances and for the unattended dots  
997 across the other factors between 15<sup>th</sup> and the 12<sup>th</sup> distances. This corresponds to the first 400 ms for  
998 the attended dots and the first 240 ms for the unattended dots after the onset (Supplementary  
999 Figure 1B). Distance decoding then dropped somewhat before ascending again as the dot  
1000 approached the deflection point. The second rise of decoding, which was more pronounced for the  
1001 attended dots, could reflect the increasing relevance to the task as the dot approached the crucial  
1002 deflection point, but it could also be due to higher visual acuity in foveal compared to peripheral  
1003 areas of the visual field. There was strong evidence that decoding of distance information for all  
1004 conditions was greater than chance (50%, BF > 10) across all 15 distance levels (Supplementary  
1005 Figure 1B).

1006



Supplementary Figure 1. Impact of different conditions in the *direction of approach* (A) and *distance to object* (B) information coding and their Bayesian evidence for difference from chance. (A) Decoding of *direction of approach* information (less task-relevant). The horizontal dashed line refers to chance-level decoding. Upper graph: Attended colour dot; Lower graph: Unattended ('distractor') colour dot. (B) Decoding of *distance to object* information (most task-relevant). Thick lines show the average across participants (shading 95% confidence intervals). Vertical dashed lines indicate critical times in the trial. Bayes Factors are shown in the bottom section of each graph: Filled circles show moderate/strong evidence for either hypothesis and empty circles indicate insufficient evidence. They show the results of Bayes factor analysis when evaluating the difference of the decoding values from chance as explained in *Methods*. Early = data from the first 5 blocks (~10 minutes). Late = data from the last 5 blocks (~10 minutes).

1007

1008

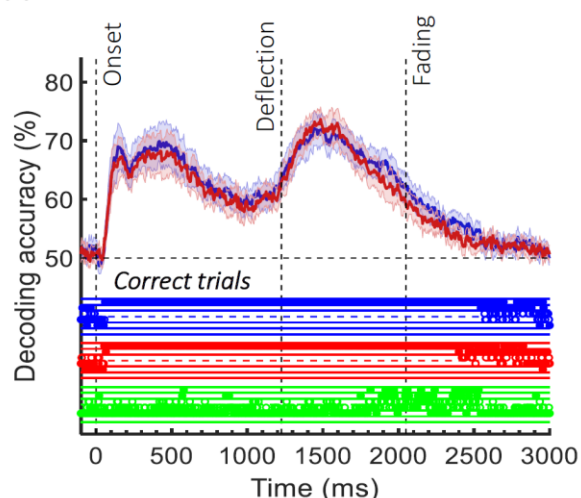
1009

1010

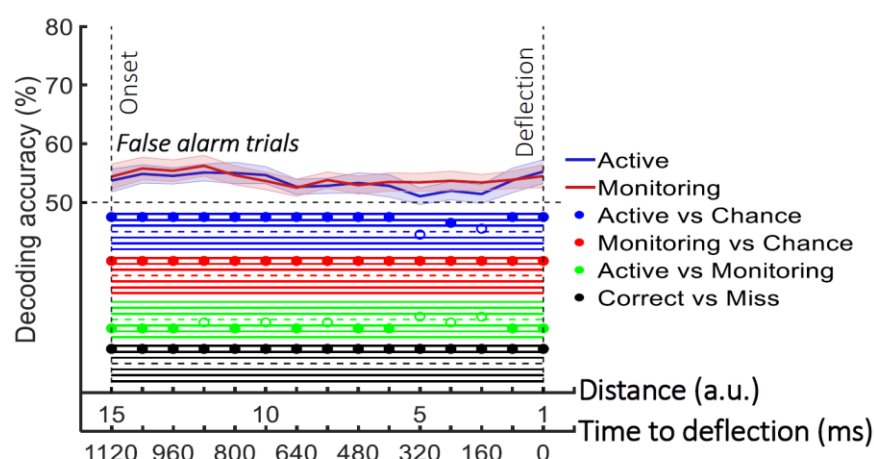
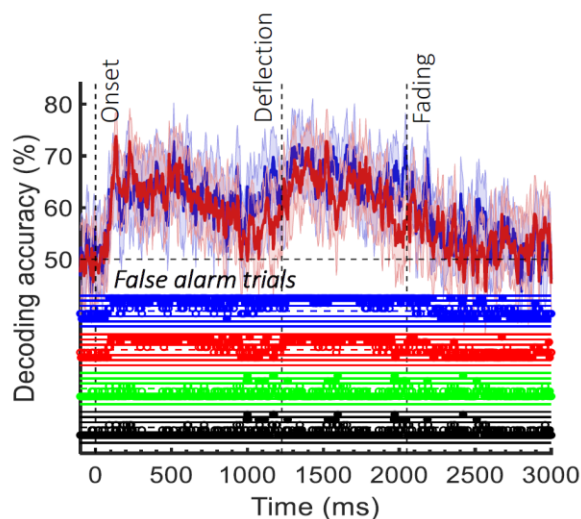
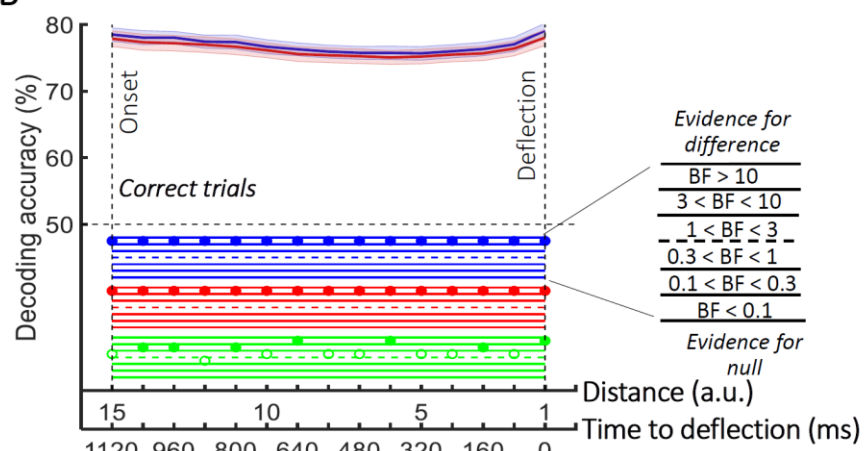
1011 Supplementary figure 2 shows the data for false alarm trials.

1012

A



B



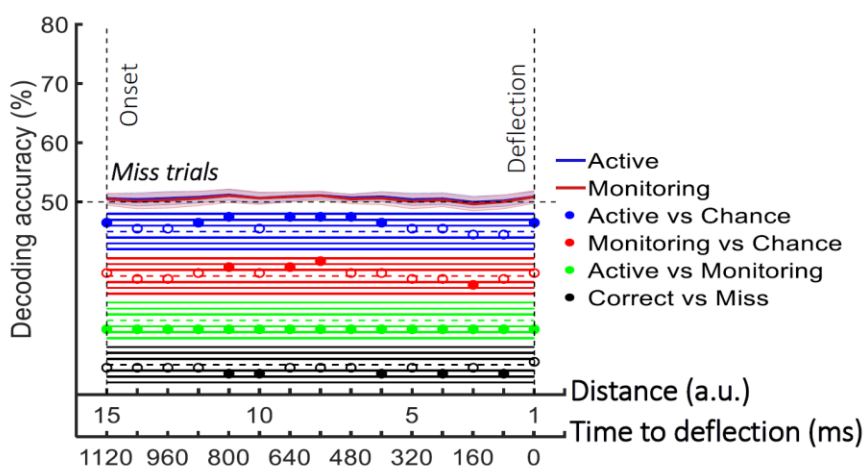
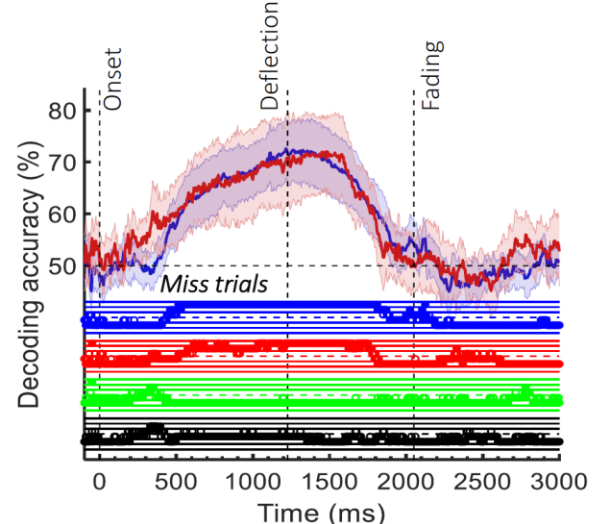
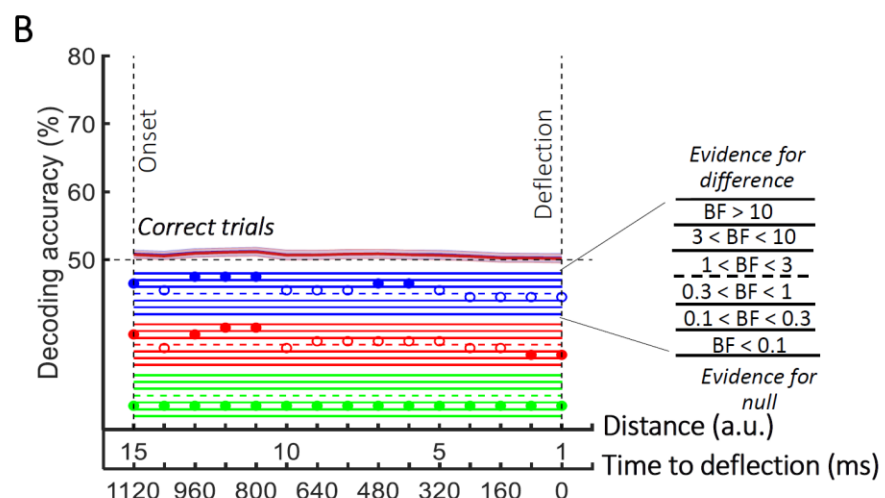
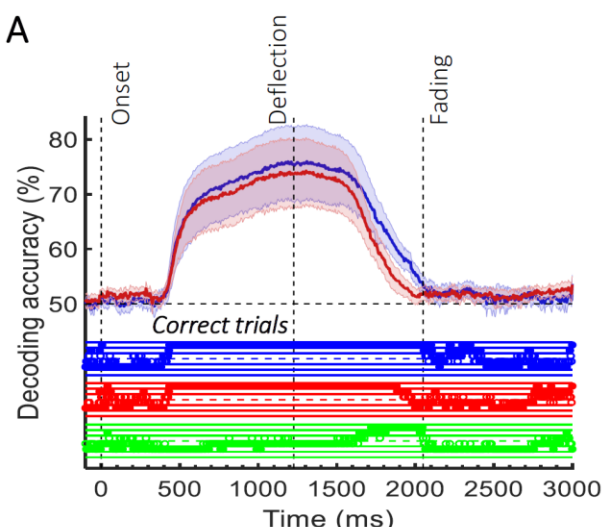
Supplementary Figure 2. Decoding of information on *correct* vs. *false alarm* trials. (A) Decoding of *direction of approach* information (less task-relevant). (B) Decoding of *distance to object* information (most task-relevant). The horizontal dashed lines refer to chance-level decoding. Top row: Decoding using correct trials; Bottom row: Decoding using false alarm trials. In both top and bottom rows, the classifiers were trained on correct trials and tested on *correct* and *false alarm* trials, respectively. Thick lines show the average across participants (shading 95% confidence intervals). Vertical dashed lines indicate critical events in the trial. Bayes Factors are shown in the bottom section of each graph: Filled circles show moderate/strong evidence for either hypothesis and empty circles indicate insufficient evidence. They show the results of Bayes factor analysis when evaluating the difference of the decoding values from chance for Active (blue) and Monitoring (red) conditions separately, the comparison of the two conditions (green) and the comparison of correct and miss trials (black). Note that for the comparison of correct and miss trials, Active and Monitoring conditions were averaged separately.

1013

1014

1015

1016 Supplementary Figure 3 shows the analysis of eyetracking data using the same  
 1017 decoding methods as for the neural data.  
 1018



Supplementary Figure 3. Decoding of information about the dot motion using the eye-tracking data. (A) Decoding of *direction of approach* information (less task-relevant). (B) Decoding of *distance to object* information (most task-relevant). The horizontal dashed lines refer to chance-level decoding. Top panels: Decoding using correct trials; Bottom panels: Decoding using miss trials. In both top and bottom panels, the classifiers were trained on *correct* trials and tested on (left out) *correct* and all *miss* trials, respectively. Thick lines show the average across participants (shading 95% confidence intervals). Vertical dashed lines indicate critical events in the trial. Bayes Factors are shown in the bottom section of each graph: Filled circles show moderate/strong evidence for either hypothesis and empty circles indicate insufficient evidence. They show the results of Bayes factor analysis when evaluating the difference of the decoding values from chance for Active (blue) and Monitoring (red) conditions separately, the comparison of the two conditions (green) and the comparison of correct and miss trials (black). Note that for the comparison of correct and miss trials, Active and Monitoring conditions were averaged separately.